Abstract

The dramatic shift in population demographics and rapid growth of the aging population has resulted in a drastic increase in the prevalence of complex age-related diseases. Of the most common age-related complex diseases, Alzheimer's disease (AD) remains the primary cause of dementia. The increased prevalence of this disease presents a major burden on our healthcare system and caregivers. Among the many pathophysiological hallmarks, there is a substantial amount of literature implicating mitochondrial dysfunction as an important signature of early AD pathophysiology. Use of 'omics' technologies and system-based approaches have become increasingly more common for studying AD. Though each data type (i.e. genomics, transcriptomics and proteomics) has advantages and disadvantages, transcriptomics serves as a cost-efficient method for obtaining a snapshot of functional molecular changes underlying the disease. Here we detail two distinct and innovative studies of the transcriptome using different analytical strategies to investigate the underlying molecular signatures of cognitive impairment in its varying forms. We report the first study of differential gene expression in mild cognitively impaired Mexican Americans. This study revealed 30 differentially expressed transcripts that were enriched for a number of biological processes previously implicated in AD pathophysiology. The second study is also the first of its kind (in the context of this phenotype) examining post-transcriptional methylation at functionally important sites within the mitochondrial transcriptome of individuals diagnosed with AD, progressive supranuclear palsy (PSP) or pathological aging (PA). We observed similar hypermethylation at these key sites in individuals diagnosed with tauopathies such as AD or PSP. Several nuclear-encoded genes were identified as associated and the expression of 5300 nuclear-encoded transcripts was correlated with this hypermethylation. These correlated transcripts were enriched for a number of biological and molecular processes. Though these studies are quite distinct in methodology, we observed overlap in the enriched processes identified in each respective study (i.e. mitochondrial dysfunction, chromatin binding/remodeling, protein degradation pathways, autophagy); many of these processes have been previously implicated in AD. Replication of these findings in larger cohorts and different racial/ethnic populations will be vital for gaining a more complete understanding of the molecular dysfunction that underlies cognitive impairment phenotypes.

TRANSCRIPTOMIC SIGNATURES OF COGNITIVE IMPAIRMENT

Dissertation submitted by

Talisa K. Silzer, MS, BSc

In partial fulfillment towards Doctor of Philosophy

Graduate School of Biomedical Science

UNT Health Science Center

July 21st, 2020

ACKNOWLEDGEMENTS

Firstly, I would like to acknowledge my major professor Dr. Nicole Phillips for her mentorship and friendship throughout my graduate school career. Her unwavering encouragement and confidence in me have helped me realize my value as a young researcher. The dedication that she shows towards her craft and her students' success is highly commendable. I would also like to thank the members of my dissertation committee with whom I've had the pleasure of working with: Dr. Robert Barber, Dr. John Planz, Dr. Vicki Nejtek and Dr. Caroline Rickards. There are also several colleagues and staff at UNTHSC that I would like to acknowledge. I would like to thank Jie Sun for having the patience to teach me a number of different wet-lab techniques. Gita, Viviana, Danielle and Courtney, thank you for being my support system and constant sounding board. I would also like to acknowledge my family. James, thank you for your patience and support throughout this process. To my Mom, thank you for your constant encouragement; you have been my cheerleader from Day-1. To Wes, thank you for always reading my work and engaging with me in scientific discussions. Finally, I would like to thank my Dad for always encouraging me to follow my passions and inspiring me to work hard.

DEDICATION

This dissertation is lovingly dedicated to my late father, Wayne Ewald Silzer. He was always very supportive of my academic journey and did his best to provide me with every opportunity to succeed in life. Though he was taken from this world too soon, I know that he would have taken great pleasure in seeing me complete this chapter. This one is for you Dad!

TABLE OF CONTENTS

LIST OF FIGURES

and PSP (purple) (bottom). Gradient bar represents gene expression level; high expression (red), low expression (blue).

Figure 12. GO terms identified as being overrepresented based on the top 1000 transcripts significantly correlated with p9 methylation at site 585. GO terms are color coded by category; Molecular function (purple), cellular component (orange), biological process (green). Terms were selected using a threshold of >2 fold change. Fold change was determined based on number of enriched genes from our 1000 transcripts list divided by the number of expected enriched genes.

Figure 13. Enriched canonical pathways based on all transcripts significantly correlated with p9 methylation. **Pathways positively and negatively correlated with p9 methylation are shown in orange and blue respectively.**

Figure 14. Hypothetical schematic of potential causes and effects of p9 methylation in neurodegeneration. **(1) Nuclear encoded genetic variants may be causal for p9 hypermethylation within neuronal mitochondria, resulting in onset or exacerbation of electron transport chain dysfunction. (2) Subsequent mitochondrial dysfunction may lead to altered downstream nuclear gene expression via retrograde signaling resulting in (3) changes to various molecular and cellular processes that further contribute to neurodegenerative pathology.**

LIST OF TABLES

ABBREVIATIONS

AD – Alzheimer's disease

Aβ – Amyloid Beta

APP – Amyloid Precursor Protein

nDNA – nuclear DNA

mtDNA – mitochondrial DNA

GWAS – Genome-Wide Association Study

mtDNACN – mitochondrial DNA Copy Number

CFmtDNA – Cell-free mitochondrial DNA

T2D – type 2 diabetes

NGS – Next Generation Sequencing

RNA-seq – RNA sequencing

HABLE – Health and Aging Brain of Latino Elders

MCI – Mild Cognitive Impairment

NHW – Non-Hispanic Whites

NC – Normal Controls

RIN – RNA Integrity Number

FDR – False Discovery Rate

IPA – Ingenuity Pathway Analysis

ANM – AddNeuroMed

mt-tRNA – mitochondrial tRNA

mt-RNA – mitochondrial RNA

PSP – Progressive Supranuclear Palsy

PA – Pathological Aging

LD – Linkage Disequilibrium

PD – Parkinson's disease

ETC – Electron Transport Chain

CHAPTER I: INTRODUCTION TO AGING AND AGE-RELATED NEURODEGENERATIVE DISEASE

With the advent of advanced medicine and improved health practices, there has been an extreme shift in population demographics. The global aging population (i.e. > 65 years) has grown quite rapidly over recent decades. In the United States, the aging population is expected to reach 95 million by the year 2060 (1). This growth poses a large burden on the healthcare system and care providers, as advanced age is associated with the onset of a number of chronic conditions including cancer, cardiovascular disease, metabolic dysfunction and Alzheimer's disease (AD).

ALZHEIMER'S DISEASE

Of the most common chronic age-related conditions, AD prevails as the leading cause of dementia in aged populations and is the sixth leading cause of mortality within the United States (2). AD is a heterogeneous disease well known for its histological hallmarks of amyloid beta (Aβ) plaque formation and tau neurofibrillary tangle accumulation, leading to synaptic loss and neurodegeneration within the brain, ultimately manifesting as behavioral changes including memory loss and inability to perform tasks of daily living. Though the disease currently affects over 5.8 million individuals in the United States, this number is only expected to grow with time. In addition, AD-related health disparities have been reported in certain racial and ethnic sub-populations; for example, African Americans and Hispanics are at 2 and 1.5X increased risk for AD respectively (2). The financial burden of the disease is significant, with an estimated $290 billion spent on treating AD patients in 2019 (2). These facts incite a need for more targeted prevention and treatment strategies for AD, a disease that currently has no cure.

Alzheimer's Disease Pathophysiology

Historically, due to the highly heterogenous nature of AD pathology, there has been significant debate concerning the primary pathophysiological features of AD and the timing of pathological onset; for a recent comprehensive review of common hypotheses, refer to (3). In brief, some of the major hypotheses regarding the primary pathological hallmarks of AD include the 1) amyloid cascade hypothesis, 2) tau hypothesis, and 3) inflammation (e.g. "inflammaging") hypothesis. In the amyloid cascade hypothesis, inappropriate cleavage of amyloid precursor protein (APP) by beta and gamma secretases produces amyloid beta peptide fragments that aggregate into plaques. The tau hypothesis proposes that the microtubule-associated tau proteins within brain axons become hyperphosphorylated leading to aggregation and tangle formation. The inflammation hypothesis is dependent on existing amyloid pathology whereby, reactive microglia and astrocytes within the brain surround existing amyloid plaques and release pro-inflammatory cytokines, further enhancing pathogenesis.

Mitochondrial Biology

Mitochondria are bean-shaped, double membrane-bound organelles located within nucleated mammalian cells that serve as key regulators of energy metabolism, cell signaling and cellular homeostasis. A single mammalian cell may contain several mitochondrial organelles; though the number is dictated by the energy demand of that tissue. The number of mitochondrial organelles is also tightly regulated through the processes of fission, fusion and mitophagy to ensure efficient functioning of the overall mitochondrial 'network' (4).

The origin of mitochondrial organelles is a complicated and highly disputed topic in evolutionary biology. Following the widely accepted endosymbiotic theory, mitochondria-containing eukaryotic cells are thought to have evolved through a symbiotic relationship

between an ancient eukaryotic host and alpha-proteobacterium (similar to the *Rickettsia* species; as shown through comparative genomics studies) (5, 6). This is supported by the resemblance of mitochondria to prokaryotes (e.g. small circular genome), The fusion of these symbiotes resulted in eukaryotic cells having two sources of genetic material: (1) nuclear DNA (nDNA) located within the nucleus, and (2) mitochondrial DNA (mtDNA) located within the mitochondrial matrix. Given the low gene content of the mitochondrial genome, the fusion event likely resulted in evolutionary reduction of mtDNA; whereby redundant genes were lost, and corresponding functions were taken over by genes encoded within the nuclear genome (6).

MITOCHONDRIAL GENETICS

Unlike nDNA which is inherited in a Mendelian fashion, mtDNA follows a non-Mendelian pattern of inheritance (i.e. maternally inherited). The mitochondrial genome replicates independently of the cell cycle and at a much faster rate compared to the nuclear genome; though mtDNA replication relies solely on nuclear encoded machinery (4). The mitochondrial proteome consisting of approximately 1500 proteins is largely reliant on nuclear genome, with very few proteins encoded by mtDNA genes (4). This complexity forces the mitochondrial and nuclear genomes to work in coordination to regulate mitochondrial bioenergetics.

Importantly, the mitochondrial genome, though haploid, is present in multiple copies; each organelle contains multiple mtDNA genomes and the number of mitochondrial genomes per cell can range from a few hundred to several thousand. In general, mitochondrial mass and relative mtDNA genome copy number is often reflective of the energetic demand of a particular cell or tissue. The multi-copy nature permits mitochondrial genomes to be homo- or heteroplasmic, which refers to the genomes having complete or incomplete sequence similarity, respectively. Due to its high replication rate, proximity to oxidative environments and lack of sufficient DNA repair mechanisms, mtDNA is highly susceptible to mutation (7). Most ‘mutations’

(or variants) within the mitochondrial genome are likely selectively neutral (8) and can be either inherited or de novo. However, the heritability of mitochondrial 'mutations' is likely dictated by random genetic drift; though the randomness of this process is a topic of debate (4). Due to the multi-copy nature of mitochondrial genomes, any given mtDNA population has the potential to be heterogeneous, meaning more than one type of mitochondrial genome (i.e. mtDNA genomes differing in sequence) is present. During oogenesis, 'mitochondrial bottlenecks' such as that shown in Figure 1, can lead to heteroplasmic alterations leading to changes in 'mutational load'. In the event that the mutation (i.e. insertion, deletion) results in loss of function, accumulation of the mutant mtDNA may increase risk for mitochondrial-related conditions or diseases (9).

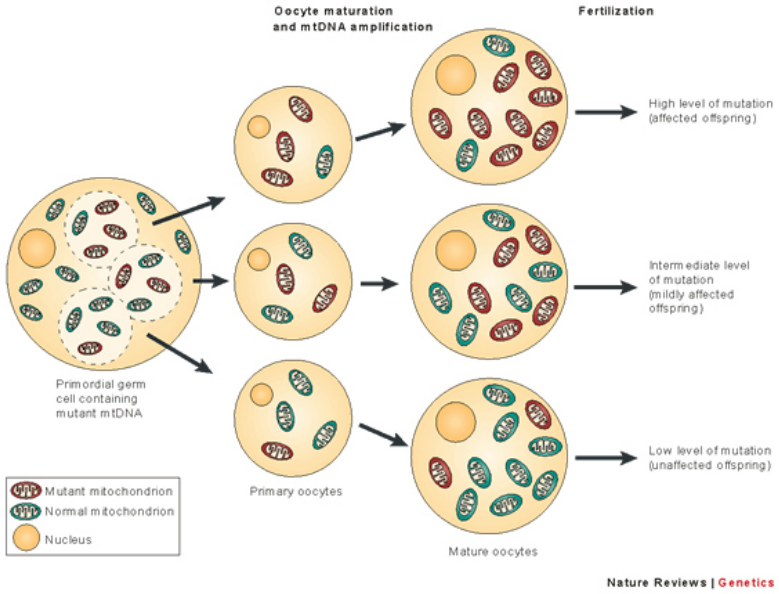

Figure 1. Mitochondrial DNA bottleneck theory. Mitochondrial genomes are selected and transferred from primordial germ cell to primary oocytes. As oocytes mature, mitochondrial DNA (mtDNA) undergoes rapid replication. This can result in mutational shifts between generations and variation in mtDNA mutations between offspring. (Image credit: Taylor, 2015. *Nature Reviews*).

Evolutionarily speaking, fixation of certain selectively neutral mtDNA variants has created stable population subgroups (termed haplogroups) that are distinguished by sequence variation. Evidence suggests that mitochondrial sequence (i.e. haplogroup) can affect metabolism and mitochondrial bioenergetics (7) and risk for human disorders. For example, the presence of one or more deleterious mtDNA mutations (i.e. m3460G>A, m11778G>A and m14484T>C) is associated with Leber's hereditary optic neuropathy, a form of bilateral blindness (4).

Mitochondrial Dysfunction in Aging and AD

Mitochondrial function is known to decline with age and since aging is an important risk factor for AD, mitochondrial dysfunction may serve as an important and early indicator of pathology. Throughout the literature, there is an abundance of evidence for mitochondrial decline in neurodegenerative disease (7, 10, 11). Different hypotheses exist concerning the role of oxidative stress and mitochondrial dysfunction in AD pathogenesis. As shown in Figure 2, the mitochondrial cascade hypothesis derived by Swerdlow et al. postulates mitochondrial dysfunction to be an upstream causal factor for AD pathology (12). In brief, inherited variation within the mtDNA sequence may determine an individual's baseline mitochondrial functionality. As mitochondrial function naturally declines with age (e.g. due to mutation or damage), surpassing of a functional threshold leads to onset of pathological/histological hallmarks of AD (i.e. plaque and tangle formation), thereby initiating a vicious cascade of events further promoting ETC dysfunction, increased ROS production and mtDNA mutations (13). It is important to note that many etiological factors contribute to onset of AD pathology, and it remains unclear whether mitochondrial dysfunction is a cause or consequence of AD pathology.

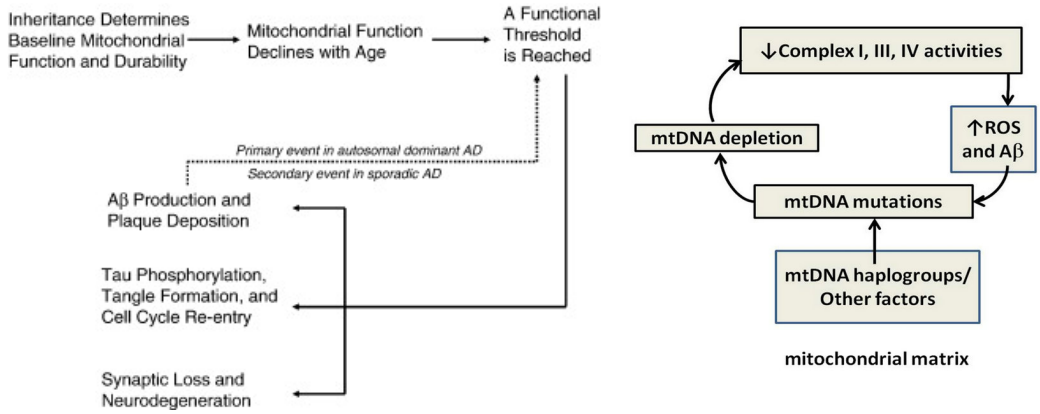

Figure 2. Mitochondrial cascade hypothesis of Alzheimer's disease. (Left image credited to Swerdlow et al., 2009; right image credited to Albrekkan and Kelly-Worden, 2013).

GENETIC SUSCEPTIBILITY FOR ALZHEIMER'S DISEASE

Late on-set AD differs greatly from the Mendelian inherited, early on-set form of the disease. AD is a highly heterogeneous disease with a complex etiology. Though several factors related to aging, environment, lifestyle and comorbid conditions have all been reported to play a role, genetics has long been recognized as an important factor in determining AD risk. Despite this, the previously reported estimations of AD heritability are variable and have historically been dependent upon study design. Some reports have suggested AD to have 74% heritability (based on a Swedish twin study) (14), while others have proposed more modest projections of 24-33% (based on GWAS findings) (15). Though several genes (e.g. *CLU*, *BIN1*, *CR1*) have been identified as having strong associations with AD risk, the *APOE* e4 allele explains approximately ~23% of the heritable risk (15); meaning that variation in risk for AD is partially attributed to this allele. *APOE* is located on chromosome 19 and encodes a lipoprotein that plays key roles in lipid transport. The effect size of the e4 allele is large in Caucasian populations, whereby individuals homozygous for the e4 allele are 10-20X more likely to develop the disease (16). Interestingly, the effect size for this allele seems to vary across racial/ethnic populations, though prevalence of the disease remains high (17). *APOE* e4 in combination with genome-wide association study (GWAS) identified SNPs has been shown to

only account for ~28% of the heritable risk for AD, and the effect associated with these variants varies across racial and ethnic groups, therefore presenting an issue of 'missing heritability' (15). This term refers to the fact that no single genetic variant can explain all of the phenotypic variation in AD risk. Though the phenomenon of missing heritability is common in studies of chronic, age-related diseases, use of non-traditional approaches as well as investigation of alternative genetic sources of risk will prove vital in increasing our understanding of AD.

Another source of potential genetic susceptibility is encoded within the mitochondrial genome. Mitochondrial dysfunction is a well-known hallmark of early AD pathogenesis. In line with the aforementioned mitochondrial cascade hypothesis, there is evidence that mitochondrial haplotypes influence risk for AD (7). For example, several different groups have reported associations between mitochondrial haplogroup H (Caucasian) and Alzheimer's disease, with some studies showing sex-based differences (i.e. females had increased risk) (7). Works published by our group have revealed significant differences in mitochondrial phenotypes in cognitively impaired individuals and related comorbidities (18, 19). These phenotypes serve as proxies for mitochondrial function; for example, mitochondrial DNA copy number (mtDNACN) is often used to assess general mitochondrial function, while cell-free mitochondrial DNA (CFmtDNA) is used to assess systemic inflammation. In a Caucasian cohort, mtDNACN was found to be significantly depressed at two different time points (4 years apart) in AD patients (19). In addition, mtDNACN was significantly lower in cognitively impaired Mexican Americans, while CFmtDNA was significantly higher in Mexican Americans with T2D; both indices were correlated with age (18).

INVESTIGATING TRANSCRIPTOMICS IN AD

The etiology and pathophysiology of AD is heterogeneous making it difficult to tease out potential causal factors. Systems-based approaches involving integration of distinct biological data types (e.g. genomics, transcriptomics, proteomics) have become increasingly more common in studies investigating the molecular underpinnings of human health and disease. Though informative, each type of 'omics' technology and its respective data have advantages and disadvantages; for a recent review, refer to (24).

Over recent decades, investigations of the transcriptome have become increasingly more common within the AD literature, which could be attributed in part, to advances in molecular technologies. A number of RNA-based technologies exist (e.g. microarray, RT-qPCR, dPCR), though Next Generation Sequencing (NGS) has become a favourable method for analyzing the transcriptome due to its high resolution. However, NGS protocols have a number of requirements including large inputs of RNA, which demands substantial amounts of high-quality cells/tissues. Since RNA sequencing (RNA-seq) serves as both a quantitative and exploratory tool, the breadth of data can be both a blessing and a curse. To further complicate things, methods and computational tools for analyzing RNA-seq data are ever evolving. For a recent review covering the many challenges of RNA-seq data analysis, refer to (25).

PROJECT OVERVIEW

The growing aging population is heavily burdened by a number of age-related diseases. Alzheimer's disease remains the leading cause of age-related dementia and prevalence of this disease within the aging population continues to grow. This presents a major concern for healthcare providers, future caregivers and potential victims of this disease. Though several genetic risk factors have been identified using genomic data, traditional GWAS and targeted gene-set analyses have yielded small effect sizes, leading to a "missing heritability" scenario. Further, investigations of the proteome have previously been limited by cost and biased techniques; though proteomic studies of AD have become more frequent over recent years. Transcriptome-based analyses are a cost-effective method for obtaining a functionally relevant snapshot of molecular changes that may be contributing to risk for cognitive impairment.

Hypothesis: Novel transcriptomic signatures underly the pathophysiology of cognitive impairment.

This hypothesis will be tested using data from two different cohorts: 1) Health and Aging Brain of Latino Elders (HABLE) and 2) Mayo RNAseq. Briefly, HABLE is a community-based study investigating biomarkers of cognitive aging and dysfunction in Mexican Americans, while Mayo RNAseq is a clinical-based study investigating transcriptomes of post-mortem brain tissue from Caucasian subjects. The following chapters examine different transcriptomic signatures of varying forms of cognitive impairment. Chapter II assesses differentially expressed genes in peripheral blood of cognitively impaired Mexican Americans enrolled in the HABLE cohort, while Chapter III investigates mitochondrial tRNA methylation in post-mortem cerebellar tissue of Caucasian subjects diagnosed tauopathies including Alzheimer's disease and progressive supranuclear palsy.

INNOVATION

Each of the following studies are distinct in how they assess transcriptomic changes underlying cognitive impairment pathophysiology (Figure 3). The first study detailed in Chapter II is the first investigation of peripheral blood gene expression profiles in Mexican Americans with mild cognitive impairment (MCI). The AD-related literature in the context of Mexican Americans is sparse; therefore, this work will be a valuable contribution towards understanding the distinct AD etiology and pathology faced by Mexican Americans. Further, the second study detailed in Chapter III is the first investigation of mitochondrial tRNA methylation in the context of neurodegenerative disease. Existing studies have investigated mitochondrial transcriptome epigenetics only in the context of healthy and cancer-related states.

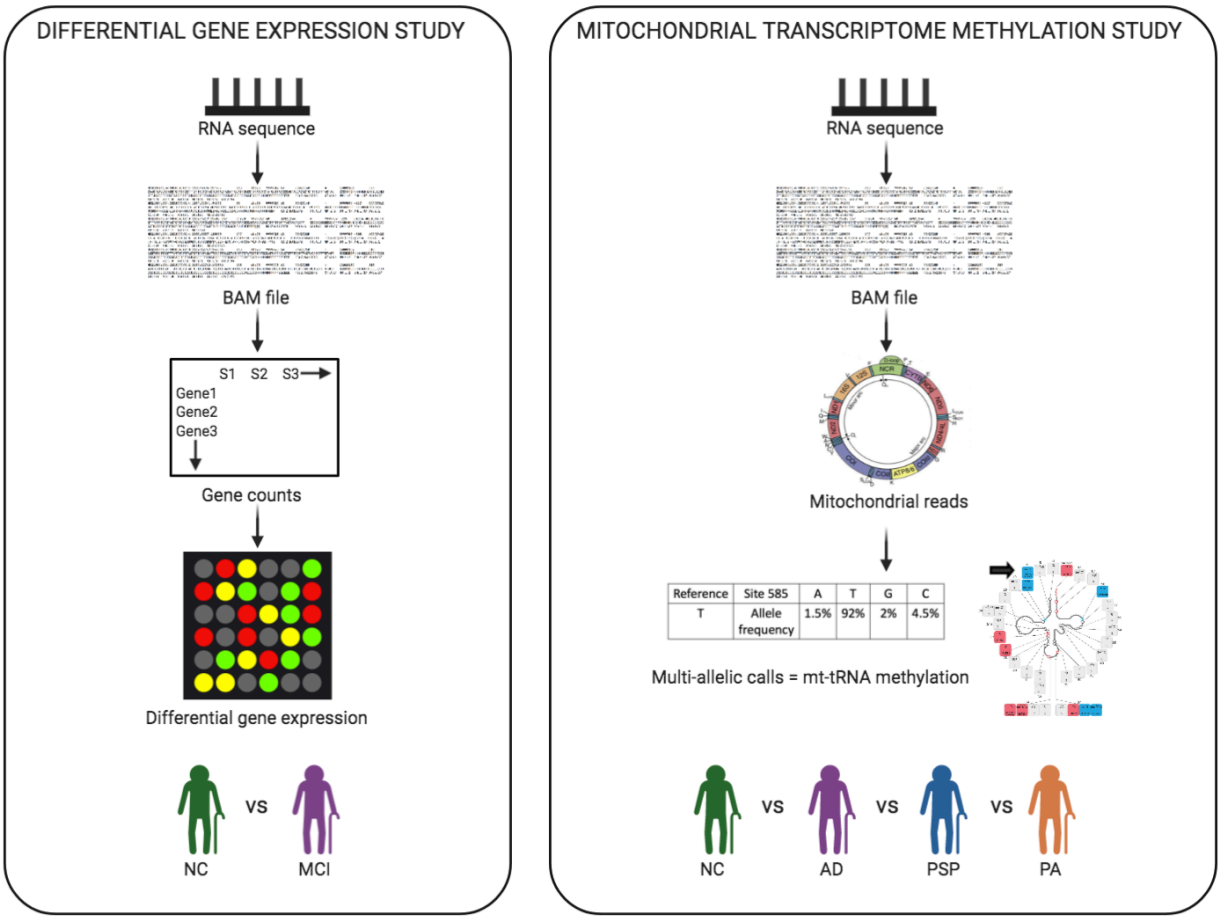

Figure 3. **Schematic detailing the general workflow for each study.** This figure was made using Biorender.

CHAPTER II: DIFFERENTIAL GENE EXPRESSION SIGNTURES IN PERIPHERAL BLOOD OF COGNTIVELY IMPAIRED MEXICAN AMERICANS

INTRODUCTION

Alzheimer's disease is the leading cause of age-related neurodegenerative dementia affecting over 5.8 million individuals in the United States alone (2). A vast proportion of the aging population of the U.S. (i.e. > 65 years of age) consists of Hispanics, primarily. Mexican Americans (62%) (26). In addition to being one of the fastest growing aging populations, Mexican Americas experience significant disparities related to late onset Alzheimer's disease (herein referred to as AD) exist in this population. Mexican Americans are known to 1) suffer from a number of comorbid conditions (e.g. metabolic dysfunction, cardiovascular disease) (27), 2) have increased risk for AD despite low frequency of APOE e4 (the largest genetic risk factor for AD among Caucasians) (27, 28), 3) experience earlier and more severe cognitive impairment (27), and 4) are often diagnosed at later stages of the disease (29). Unfortunately, Mexican Americans are underrepresented in the medical literature and etiology of these AD-related health disparities remains poorly understood.

Blood based biomarkers for AD have been a focus of investigation for several groups over recent years (30). Our group has previously identified protein biomarkers for distinguishing AD cases from controls in both Hispanics (i.e. Mexican American) and Non-Hispanic Whites (NHW) (27, 31). Based on our past findings, Mexican Americans appear to experience AD pathophysiology that is more metabolic in nature compared to the inflammatory type of AD experienced by NHWs. These results were further corroborated by our group in a recent epigenomic study of Mexican Americans with vs. without cognitive impairment that identified

differentially methylated sites and regions within the genome that were linked to metabolic dysfunction and inflammation (32).

Within the AD literature, there are few studies exploring differential gene expression in peripheral blood. Blood based gene expression profiles are potentially valuable non-invasive and ethnicity-specific biomarkers for predicting onset or severity of cognitive impairment. Here using peripheral blood from Mexican American participants enrolled in a cognitive aging cohort we sought to 1) identify differentially expressed genes in MCI, 2) determine what downstream cellular and/or molecular processes may be altered and 3) identify how these changes may differ from those previously reported in populations of European-ancestry. With MCI serving as a clinical precursor for AD, it is important to establish overlap in molecular signatures, as this may aid in identification of individuals who are likely to transition from MCI to AD-related dementia.

METHODS

SAMPLE OBTAINMENT

This study was approved under the North Texas Regional IRB #2012-083. All participants in this study and/or their legal guardian, gave written consent. Fasted-state peripheral blood buffy coats were obtained from 50 Mexican American participants enrolled in the Health and Aging Brain of Latino Elders (HABLE) study, a community-based cognitive aging cohort. Participants were either normal controls (NC) or diagnosed with MCI (Table 1). Across groups, participants were matched pair-wise based on age (± 5 years), sex and hypertension. Phenotypic information was collected via interview. A detailed description of methods used for blood and phenotype collection has been previously reported (32).

Table 1. Demographics of the Mexican American participants utilized in this study.

	NC (n=24)	MCI (n=26)	p-value
Age	63.54 ± 7.43	64.27 ± 7.96	0.739
Sex (Female:Male)	18:6	20:6	0.877
Education	8 ± 4.82	5.54 ± 3.95	0.056
Hypertension (%)	79	92	0.197
RIN	5.05 ± 0.97	4.16 ± 1.57	0.026

Hypertension is specified as percentage of cases. P-values are based on student t-test.

RNA EXTRACTION AND SEQUENCING

Peripheral blood samples were handled in accordance to the UNTHSC Institutional Biosafety Committee approved protocol IBC-2018-0078. RNA was extracted from peripheral blood buffy coat using the TRIzol Plus RNA purification kit. RNA extracts were QC'd using the Qubit fluorometer. RNA integrity (RIN) values were obtained using the Agilent 4200 Tapestation and RNA screentape; average RIN score across all samples was 4.57. The sub-optimal RIN scores can be attributed to the degraded nature of the samples; blood samples were frozen for several years in the absence of any RNA preservatives. Globin RNA was removed using the GLOBINClear™ Human kit (Thermo Fisher Scientific, Waltham, MA). With the globin-depleted RNA extracts, sequencing libraries were prepared using the Illumina TruSeq Total RNA kit (Illumina, San Diego, CA) following manufacturer's instructions. Libraries were single-end sequenced in quadruplicate (4 lanes/per sample) on an Illumina HiSeq2000 instrument. Average sequence length was approximately 75bp.

DATA ANALYSIS

Raw RNA sequence data (fastq format) were QC'd using FASTQC (33). RNA sequences were aligned and quantified using Salmon and a decoy-aware transcriptome index (based on Ensembl 97); the mapping-based index was built based on 31 k-mer length. Differential expression analysis was conducted on the non-normalized Salmon-derived gene counts using DESeq2 in R. Internal data normalization was performed in DESeq2 using EstimateSizeFactors; this divides read counts for each gene by the geometric mean for the same gene across all samples and accounts for library size and RNA composition (34). Two samples were removed prior to differential expression analysis due to outlying read counts; this yielded a final sample size of 48. DESeq2, which utilizes a generalized linear model, was used to identify significantly differentially expressed genes (34). Though found to be significantly different between NC and MCI groups, RIN scores were not incorporated as a covariate in the model. Similar to the results of a controlled degradation experiment (35), our RNA extracts all displayed comparable RIN values (RIN values were normally distributed) suggesting that all samples were likely degraded in an equivalent linear fashion over time. The threshold applied for identifying significantly differentially expressed genes was an FDR adjusted p-value less than 0.05 and log2 fold change greater ±2. Differentially expressed genes were annotated in R using the 'ensembl' mart as part of the bioMart package (36). Pathway and GO enrichment analyses were performed using IPA (QIAGEN Inc.) and ShinyGO (37) which both utilize Fisher's Exact test. IPA information can be found at: https://www.qiagenbioinformatics.com/products/ingenuitypathway-analysis. Protein interaction networks were generated using STRING v.11 (38).

RESULTS

Here we examined gene expression profiles of peripheral blood from Mexican American participants enrolled in a Texas cognitive aging cohort (HABLE). We identified numerous transcripts that were differentially expressed when comparing normal vs. MCI; 30 transcripts survived FDR correction (Table 2).

Table 2. Differentially expressed transcripts in MCI.

Ensembl Transcript	HGNC Gene	Log2 Fold Change	P-value	Adj. P-value
ENST00000320868.9	HBA1	-27.15208385	1.29E-20	1.95E-16
ENST00000617821.4	NKTR	-26.59016657	3.71E-28	1.88E-23
ENST00000448507.5	TBC1D14	-25.64542279	9.36E-33	7.09E-28
ENST00000509903.5	CAST	-24.94715367	5.71E-34	8.66E-29
ENST00000611640.4	KDM4B	-24.61317367	3.93E-27	1.49E-22
ENST00000652462.1	ITGB2	-23.61996134	5.70E-16	4.32E-12
ENST00000540442.5	ORC4	-23.55183527	6.91E-16	4.76E-12
ENST00000395878.8	UBFD1	-23.38252026	4.44E-17	5.18E-13
ENST00000084795.9	RPL18	-23.36820861	6.75E-16	4.76E-12
ENST00000317336.11	ODF2L	-23.34162994	5.66E-17	5.90E-13
ENST00000520553.5	HCK	-22.94287892	3.79E-15	2.39E-11
ENST00000263285.11	LY9	-22.88679217	9.74E-17	8.69E-13
ENST00000650810.1	MXI1	-22.61857887	9.23E-15	5.38E-11
ENST00000422452.2	TENM1	-22.35017359	1.91E-14	1.07E-10
ENST00000360839.7	ANKHD1	-22.13706886	3.40E-14	1.78E-10
ENST00000453091.6	RIF1	21.89098226	7.15E-14	3.62E-10
ENST00000564831.6	APOBR	21.97867268	1.55E-18	2.13E-14
ENST00000000412.8	M6PR	22.3165498	2.27E-14	1.23E-10
ENST00000615872.4	MBOAT7	22.7242354	7.44E-15	4.52E-11
ENST00000359709.7	IFI16	22.77604782	3.39E-16	2.71E-12
ENST00000435768.6	ATF6B	23.15030782	9.50E-17	8.69E-13
ENST00000324210.9	MBNL1	23.55735604	7.27E-16	4.79E-12
ENST00000396029.8	ADNP	23.76318149	1.56E-16	1.32E-12
ENST00000468435.6	UHRF2	24.12492143	9.00E-27	2.28E-22
ENST00000357327.9	TNIK	24.2207215	5.84E-17	5.90E-13
ENST00000556428.5	SNW1	24.24367321	1.36E-26	2.95E-22
ENST00000428775.1	PRRC2A	24.31121384	1.29E-21	2.18E-17
ENST00000262585.6	DENND3	24.45621209	1.16E-21	2.18E-17
ENST00000422962.1	PRRC2A	24.6933156	8.51E-27	2.28E-22
ENST00000653979.1	TPM4	24.86228053	1.65E-17	2.09E-13

Adjusted p-value was calculated using the Benjamini-Hochberg procedure.

These 30 transcripts mapped to 29 unique genes; 15 genes were down-regulated and 14 were up-regulated. In IPA the differentially expressed gene-set was tested for enrichment for canonical pathways using the Core analysis tool. This analysis revealed a number of processes to be enriched including Reelin Signaling in Neurons, CDP-diacylglycerol Biosynthesis and Phosphatidylglycerol Biosynthesis (Figure 4; Appendix 1).

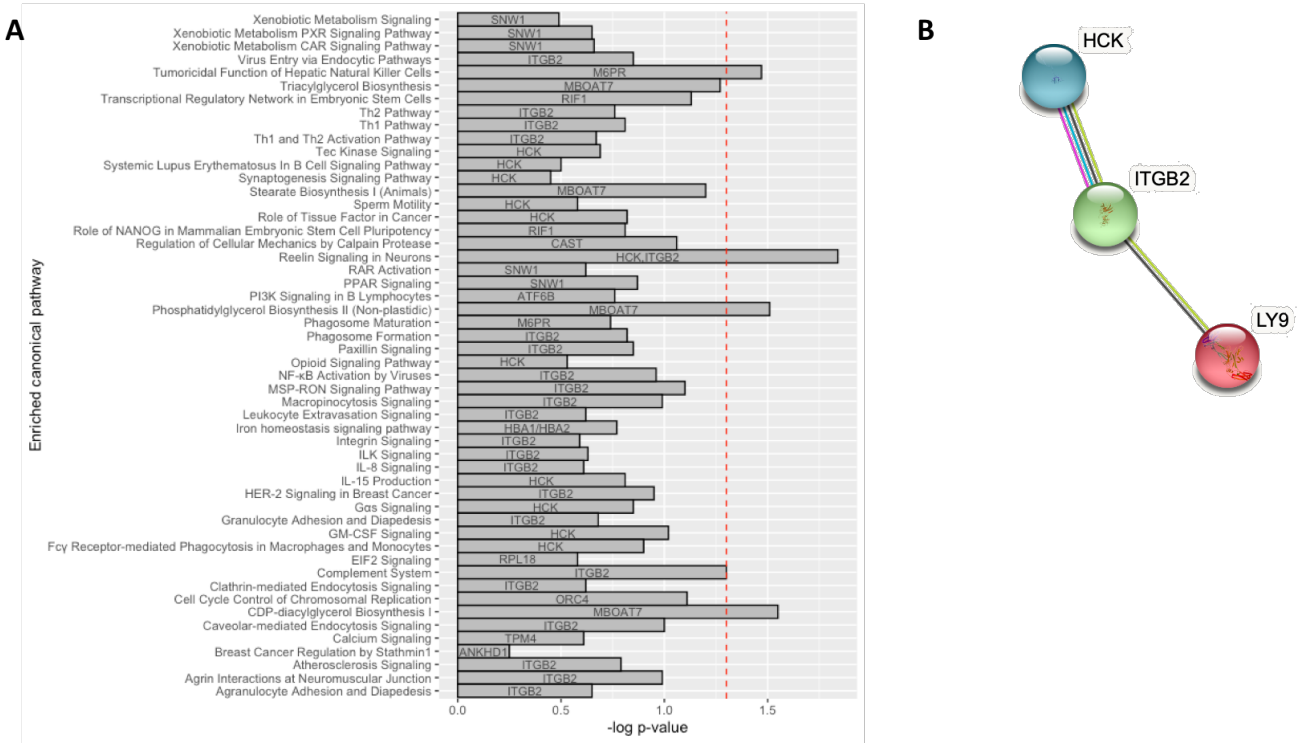

Figure 4. Enriched IPA canonical pathways based on the differentially expressed gene-set. A) Bar plot displaying enriched pathways. Significant pathways are shown on the y-axis, while level of significance (shown as -log p-value) is shown along the x-axis. Red line indicates threshold (p-value of 0.05). B) Protein interaction network associated with reelin signaling. Lines are indicative of findings; co-expression (black), experimental (pink), database (blue) and text-mining (green).

To further elucidate the biological directionality of these changes, we tested for enrichment in the up- and down-regulated gene-sets separately using ShinyGO. Though the down-regulated gene-set yielded no significant enrichment, the up-regulated gene-set showed enrichment for a number of functional processes including endolysosomal processing, regulation of histone modifications, chromatin remodeling, mRNA splicing and processing as well as apoptosis (Figure 5; Appendix 2).

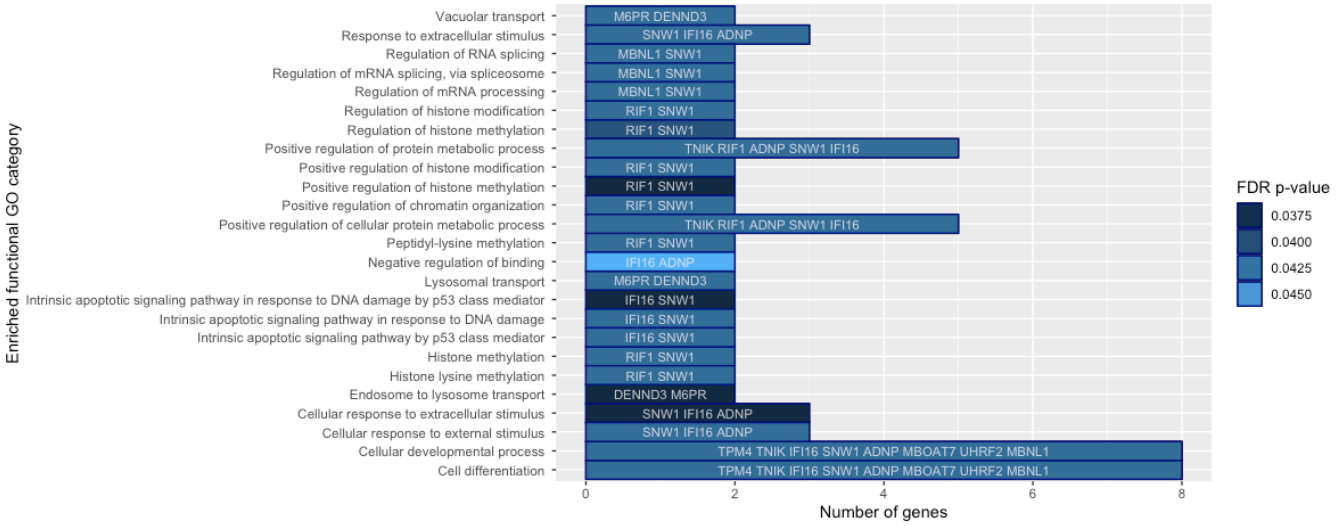

Figure 5. Enriched ShinyGO biological functions based on the up-regulated gene-set. Significant processes are shown along the y-axis, while the number of genes associated with each process is shown along the x-axis. Specific genes associated with each process are labelled. Color of each bar is indicative of FDR adjusted p-value.

DISCUSSION

Within the AD literature, it has become clear that the origin of cognitive impairment experienced by Mexican Americans is generally distinctive from that of Non-Hispanic Whites (NHW). These differences and the observed AD disparity in Mexican Americans, is partially attributed to the high prevalence of metabolic dysfunction within Mexican American populations, with up to 46% of Latinos suffering from comorbid dementia and diabetes (39). Other genetic and socioeconomic factors may also contribute to the disparity. As mentioned in previous

publications by our group, there is limited literature regarding AD in Mexican American populations (32). In the general AD literature, no groups have investigated differential gene expression in peripheral blood; the vast majority of studies have focused on tissue-specific (i.e. brain) gene expression. This is one of the first studies investigating peripheral blood gene expression of Mexican Americans with or without MCI. Since MCI generally precedes AD, increasing our understanding of the underlying biological and molecular changes in MCI, particularly in understudied populations (i.e. Mexican Americans), could have major implications on how disease progression is monitored and potentially facilitate the identification of individuals most likely to convert (i.e. individuals with MCI who may transition into AD-related dementia).

CANONICAL PATHWAY ENRICHMENT FOR DIFFERENTIALLY EXPRESSED GENES IN MCI

In this study of RNA sequence data from peripheral blood of Mexican American participants, we identified 30 differentially expressed transcripts, many of which have previously been directly or indirectly (i.e. via biological processes) associated with AD. Using the differentially expressed gene-set, we tested for enrichment for biological processes and pathways in IPA; this yielded four enriched canonical pathways, three of which have been linked to AD (Figure 4; Appendix 1). The most significantly enriched pathway was *Reelin Signaling in Neurons*. Reelin is an extracellular matrix glycoprotein well known for its role in neuronal migration and positioning in the developing human brain. Within the aging brain, reelin serves as an important regulator of synaptic plasticity, likely through modification and maintenance of dendritic spine morphology (40). Distinct expression patterns in different brain regions of murine models suggests that reelin signaling may also play crucial roles in learning and memory (40). Within human AD brains, unique N-terminal forms of reelin have been shown to aggregate and colocalize with amyloid beta (Aβ) (40). Genes in our dataset with connections to reelin signaling and microglial dysfunction include *HCK*, *ITGB2* and *LY9* (Figure 1B). Microglial dysfunction is a

common hallmark of AD pathology (41) and contributes to the 'inflammaging' phenotype commonly seen in AD patients. *HCK* encodes a hematopoietic cell kinase that functions as a regulator of phagocytosis. Expression of *HCK* has been reported to be altered in AD brains (42) and knock-down of *HCK* has been proposed to accelerate AD-like neuropathology via microglial dysregulation (43). Differential expression of *LY9*, encoding a T-cell surface antigen, has also been previously implicated in a microglial-type neurodegeneration in mice (44). Further, *ITGB2*, encoding integrin subunit beta 2 protein, has been observed to be differentially expressed in AD brains (45). Though it is somewhat unclear what role reelin signaling (and these genes) may be playing in the periphery, ITGB2 is known to coat blood leukocytes and plays a critical role in recognition of inflammatory signals and mediates subsequent binding of leukocytes to blood vessel walls. Further, pro-inflammatory gene expression has been observed to be up-regulated in peripheral myeloid cells in patients with MCI or AD (46). These findings in peripheral blood may be indicative of systemic inflammation related to cognitive impairment pathology.

Another IPA pathway found to be enriched in our differentially expressed gene-set was CDP-diacylglycerol Biosynthesis. CDP-diacylglycerol is a known glycerolipid intermediate involved in phosphatidylinositol and cardiolipin synthesis. Though both phosphatidylinositol and cardiolipin have complex functions, their primary roles relate to signal transduction and mitochondrial function/morphology respectively (47). Dysregulation of lipid homeostasis and biosynthesis has been associated with aging and AD pathogenesis. For example, diacylglycerol (DAG) levels have been observed to be elevated in patients diagnosed with MCI (based on measurements from frontal cortex and blood plasma) (48). This elevation may contribute to inflammation, as well as amyloidogenesis (49). Importantly, disruption to cardiolipin synthesis (which takes place within the mitochondria) has critical ramifications on mitochondrial function and AD pathology (50) and is another area of investigation for our group (18, 23). Phosphatidylglycerol biosynthesis was also found to be enriched in our differentially expressed

gene-set; phosphatidylglycerol is not well researched in the context of AD but it is directly linked to cardiolipin synthesis. Previous work by Wood et al. has shown elevated levels of phosphatidylglycerol metabolites in blood plasma of cognitively impaired patients (51). Together, ours and previous findings indicate that key molecular indicators of metabolic dysfunction are detectable in the peripheral blood and may be early signs of cognitive impairment; our recent work investigating epigenetic changes in the peripheral blood support this notion as well, based on methylation profiles (32).

BIOLOGICAL PATHWAY ENRICHMENT FOR UP-REGULATED GENES IN MCI

In the up-regulated gene-set, we observed enrichment for a number of biological/molecular functions (Figure 5, Appendix 1). Several of the enriched GO terms were related to chromatin modifications and organization (i.e. *Positive regulation of chromatin organization, Regulation of histone methylation*). RIF1 (replication timing regulatory factor 1) has a well-documented role in telomere maintenance and regulation of DNA replication and double strand break repair pathways (52). It also controls chromatin reorganization; for example, *RIF1* depletion has been shown to cause increased chromatin loop size, resulting in major transcriptional changes (based on mouse embryonic stem cells) (53). SNW1 (SNW domain-containing protein 1) is a coactivator known for enhancing transcription and also plays a role in RNA processing via interaction with spliceosome complexes. In addition, histone demethylase *KDM4B* was observed to be down-regulated in our gene-set. In *Drosophila melanogaster* declines in *KDM4B* (as shown by knockout model) have been shown to ameliorate neurotoxic effects of tau through restoration of heterochromatin (54). Enrichment for RNA processing and splicing was also observed in the up-regulated gene-set. Though the GO terms specified are rather generic and difficult to interpret in this context, several of the aforementioned processes have been previously identified in peripheral blood of AD patients enrolled in the AddNeuroMed

(ANM) 1 and 2 consortia (55). Interestingly, genes encoding ribosomal proteins (e.g. *RPL18*) have also been previously identified as differentially expressed in both blood and brain tissue of AD subjects (56). Though it is challenging to interpret the biological significance of these enriched processes, there is evidence to suggest that histone modifications may have the ability to regulate RNA splicing through direct interaction with the spliceosome (57).

Processes related to endolysosomal processing/transport and apoptosis were also found to be enriched in the up-regulated gene-set. Further, *ANKHD1* encoding an anti-apoptotic protein, was observed to be down-regulated. This gene has been previously implicated in both AD and ischemic stroke based on gene-based GWAS (58). This implicates two different death mechanisms in MCI. Disentangling the complex interactions between apoptotic and autophagic players is difficult. Evidence suggests that the processes of autophagy and apoptosis may be capable of regulating one another (59). Dysregulation of the endo-autolysosomal system is common in tauopathies such as AD, with accumulation of endo and auto-lysosomal structures serving as hallmarks of pathology (60). For example, accumulation of immature autophagic vesicles is a common feature of AD pathophysiology and may result in lack of clearance and/or buildup of tau and Aβ (61), though reports of this have been varied in peripheral blood (62).

Lastly, cell development and differentiation were enriched in the up-regulated gene-set. Synaptic dysfunction is a well-known feature of AD-related brain pathology. Within human AD brains, hippocampal neurogenesis has been shown to be up-regulated, likely as a means to replace damaged neurons (63). However, given that our observations were made in peripheral blood leukocytes, interpretation of our findings is complicated. Leukocytes are generally considered to be cells of the periphery; however, it is unclear how their development or differentiation may be playing a role in cognitive impairment pathophysiology. There is evidence to suggest that leukocytes may infiltrate the brain upon stimulation by Aβ (64), though more

studies are needed to fully understand the ability of leukocytes to cross the blood brain barrier and the role they may play within the brain.

OTHER DIFFERENTIALLY EXPRESSED GENES LINKED TO COGNITIVE IMPAIRMENT

A number of other genes within our differentially expressed gene-set were identified as being previously associated with AD. *CAST* (*calpastatin*) encodes a calpain inhibitor that is closely linked to proteolysis of Aβ. Depletion of CAST has been reported in AD brains and is hypothesized to contribute to dysfunctional calpain activity leading to synaptic dysfunction and subsequent neurodegeneration (65). Calpain has also been linked to tau processing; particularly, calpain-mediated cleavage leads to unique tau fragments that can localize to and inhibit mitochondrial function (66).

Further, we observed up-regulation of *APOBR*, which encodes the apolipoprotein B receptor protein which is primarily responsible for processing dietary lipids. The corresponding ligand APOB has been observed to be up-regulated in peripheral blood sera of AD patients and plasma of MCI patients, suggesting that apolipoproteins (and their corresponding receptors) other than APOE may be involved in cognitive impairment pathology (67, 68). Additionally, *PRRC2A* encoding proline rich coiled-coil 2A was identified as up-regulated; this gene has previously been implicated on a gene predictive gene panel for distinguishing normal controls from MCI and/or AD (AUC >0.6) in the ANM cohort (69).

CONCLUSION

The results presented here point to dysregulation of several biological and molecular processes linked to AD pathology among Mexican Americans, including inflammation, cell development/differentiation, cell death, chromatin regulation via epigenetic modifications and

RNA processing (Figure 6). Though the enriched terms are somewhat vague, it is interesting that we detected AD-associated changes in peripheral blood of MCI patients. Based on the reported findings, we hypothesize that systemic inflammation may be causing up-regulation of cell death mechanisms such as apoptosis and autophagy. Further, synaptic dysfunction is a known feature of AD pathology. The enrichment observed for cell development/differentiation may be reflective of compensatory neurogenesis within the brain; though what this finding may be pointing to in the periphery is unclear. Lastly, epigenetic changes are common in both aging and age-related diseases such as AD. Here we postulate that changes to chromatin structure via histone modifications may in fact be communicating with RNA splicing machinery to influence downstream gene expression (57).

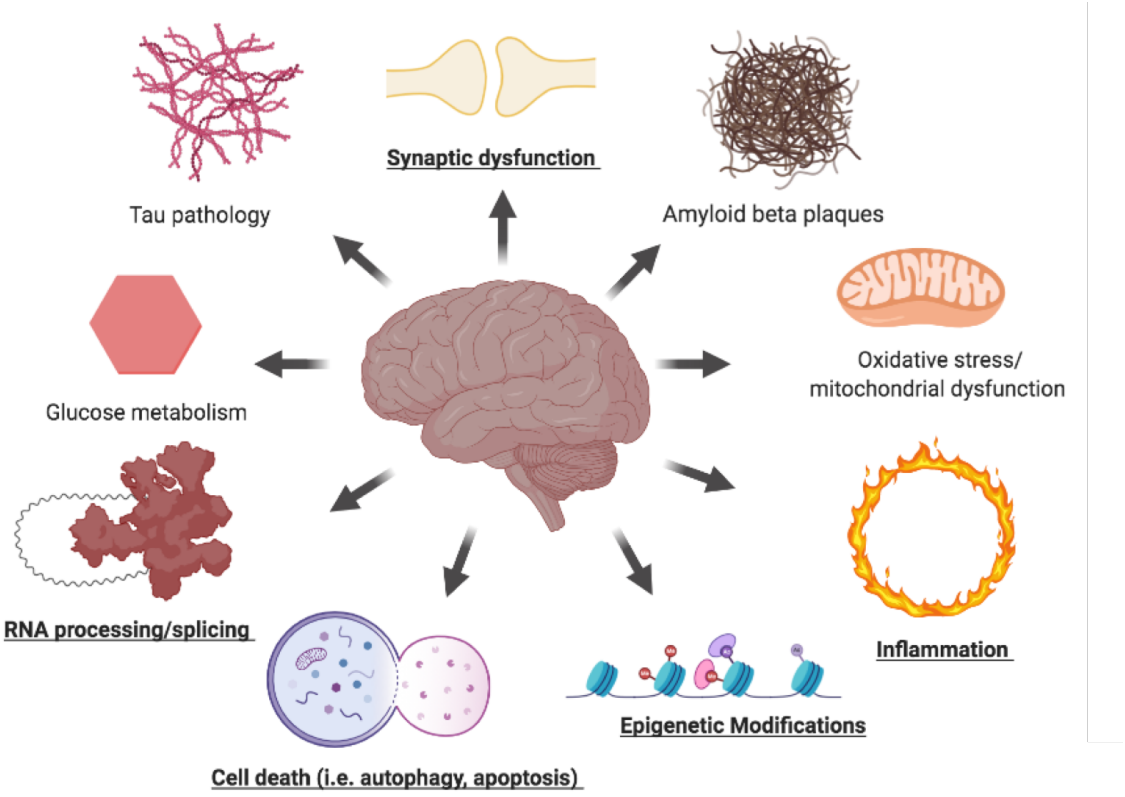

Figure 6. Schematic diagram detailing common molecular signatures of Alzheimer's disease. The molecular features shown here are not an exhaustive list. Bolded terms represent processes identified as enriched in our dataset. This illustration was created using BioRender.

Though we identified several differentially expressed transcripts were linked to cognitive impairment and AD pathology, it is important to acknowledge the limitations of the current study. Firstly, the sample size is small, therefore all genes identified here should be considered as preliminary results. Future studies will be directed at replicating these results in a larger cohort and comparing differentially expressed genes between Mexican Americans and NHWs to identify potential overlap or divergence in molecular signatures. Further, cognitive impairment is a condition that primarily affects regions of the brain. Here we focused on molecular signatures of peripheral blood. Though we acknowledge that gene expression changes in peripheral blood are not a direct measurement of what may be occurring within the brain, previous studies by our group suggests that blood based biomarkers can be quite accurate in detecting AD both in NHWs and Mexican Americans (31, 70). Of note, the nature of the samples used here may have also influenced our findings. The peripheral blood samples were stored at -80 °C for several years in the absence of any RNA preservative, which is likely the cause of the low RIN values observed. Although bioinformatic processes for normalizing reads should help to account for differences in RIN, it is likely that our results reflect only differential expression for those transcripts that are most abundant in peripheral blood and resistant to degradation. Ideally, future studies would entail extracting RNA from fresh blood tissue to allow for optimal RNA quality, though unfortunately this is often not feasible when capitalizing on the invaluable samples that have been collected through historical biobanking initiatives.

Despite these limitations, we strengthened our study design and analysis by 1) selecting demographically balanced experimental groups that were representative of the Mexican American population and 2) normalizing our RNA count data based on read depth, allowing for more accurate detection of differentially expressed genes. Our study has identified AD-related gene expression signatures of peripheral blood in Mexican Americans diagnosed with MCI.

Further studies are needed to aid our understanding of the AD-related health disparities faced by Mexican Americans.

ACKNOWLEDGEMENTS

The research team thanks the local Fort Worth community and participants of the Health & Aging Brain Study. Research reported in this publication was supported by the National Institute on Aging of the NIH under Award Numbers R01AG054073 and R56AG054073. We would also like to acknowledge the National Institute on Minority Health and Health Disparities of the NIH under award number 3U54MD006882-08S2 for supporting this research. The content is solely the responsibility of the authors and does not necessarily represent the official views of the National Institutes of Health.

Chapter II Noteworthy Results

- Differential gene expression is detectable in peripheral blood
- Differentially expressed genes point to inflammation, cell death, cell differentiation, epigenetic modifications and RNA processing underlying mild cognitive impairment
- Molecular signatures of mild cognitive impairment overlap with previously reported findings in Alzheimer's disease

CHAPTER III: MITOCHONDRIAL TRNA METHYLATION IN ALZHEIMER'S DISEASE AND PROGRESSIVE SUPRANUCLEAR PALSY

INTRODUCTION

Though it has traditionally been recognized that modifications to or variations within nuclear and mitochondrial DNA can critically alter mitochondrial function, few investigators have explored the potential implications of transcriptomic modifications. Unlike modifications to DNA where gene expression is directly affected, modifications to RNA critically impact efficiency of translation and protein synthesis. A growing body of evidence suggests that within the mitochondrial transcriptome specifically, key modifications at certain sites within mitochondrial tRNAs (mt-tRNAs) have significant impact on mitochondrial RNA (mt-RNA) translation. Of the most common modification types, methylation at the ninth position (termed 'p9 site') of mt-tRNAs appears to have functional consequences by altering the folding, stability and decoding capacity of mt-tRNAs (71-74). At position nine within the cloverleaf tRNA structure, methyl groups are added to adenosine by mitochondrial ribonuclease P protein 1 (MRPP1) yielding 1-methyladenosine (m1A). Evidence suggests that basal levels of p9 methylation is required for proper tRNA processing (73). It is unclear what the functional consequence of hyper- or hypo-methylation is; however, lack of methylation at this site has been associated with rare neurodegenerative disorders such as HSD10 disease (75). Further, knockdown of processing molecules such as MRPP1 has been shown to disrupt tRNA processing leading to declines in mitochondrial protein synthesis (76).

Previous studies by other groups have explored p9 methylation in the context of human health (77) and cancer (78). In a sequence-based study focused on a non-diseased French-Canadian cohort (CARTaGENE), the mitochondrial transcriptome was shown to be highly

polymorphic (77). Of note, 13 sites within the mitochondrial transcriptome were observed to be multi-allelic (i.e. containing three or more nucleotides at a single position), a common signature of reverse transcription errors during cDNA synthesis. These sites were also discovered to overlap with regions known to be post-transcriptionally modified (77). An association between *MRPP3* and multiallelic variability was identified through GWAS, suggesting that genetic variants may influence the rate of post-transcriptional methylation in human mitochondria (77). In a follow-up study investigating human cancer, the authors observed p9 site hypermethylation in tumor tissues from multiple cancer types (when compared to normal tissues); the rate of methylation appeared to correlate with patient survival outcomes (78). Genotype-disease interactions were also identified, suggesting that, within a disease context, nuclear variants may impact an individual's ability to maintain stable methylation marks at these specific sites (78). Interestingly, this concept has not yet been investigated in the context of cognitive impairment, a highly heterogeneous condition in aging populations. Here, we sought to explore the potential role for mitochondrial transcriptome methylation in the context of two different tauopathies (i.e. Alzheimer's disease and progressive supranuclear palsy) and identify upstream or downstream factors associated with this modification.

METHODS

SAMPLE DESCRIPTION

Post-mortem cerebellar tissue of 266 Caucasian subjects from the Mayo Clinic Brain Bank and Banner Sun Health Research Institute were originally collected for the Mayo RNAseq study led by Dr. Nilüfer Ertekin-Taner, Mayo Clinic, Jacksonville, FL as part of the multi-PI U01 AG046139 (MPIs Golde, Ertekin-Taner, Younkin, Price). Subjects were either healthy or diagnosed with Alzheimer's disease (AD), progressive supranuclear palsy (PSP) or pathological aging (PA). For details regarding diagnosis, refer to doi:10.7303/syn5550404.

Table 3. Demographics of subjects used.

Diagnosis	Sex	Age at Death	APOE		
			e2	e3	e4
NC (n = 74)	Male (n = 40)	80.93±8.15	7.43%	86.40%	6.08%
	Female (n = 34)	85.15±6.76			
AD (n = 82)	Male (n = 34)	81.68±8.17	2.44%	68.30%	29.30%
	Female (n = 48)	83.21±7.19			
PSP (n = 83)	Male (n = 51)	74.22±6.94	9.04%	82.53%	8.43%
	Female (n = 32)	73.65±5.99			
PA (n = 27)	Male (n = 11)	85.18±3.74	7.41%	75.92%	16.67%
	Female (n = 16)	84.06±4.65			

Age is reported as an average ± standard deviation for each respective group. Normal control (NC), Alzheimer's disease (AD), progressive supranuclear palsy (PSP), pathological aging (PA).

DATA ACQUISITION AND QUALITY CONTROL

SNP, RNA-seq and gene expression data were acquired from the Synapse data repository (doi:10.7303/syn5550404). Briefly, genotypes were obtained using the Illumina Human Omni 2.5Exome array. SNP data was QC'd in PLINK to exclude individuals based on relatedness, discrepant sex information, low genotyping call rate (<98%) and extreme heterozygosity (± 3 standard deviations from the mean) (79). EIGENSTRAT was utilized to identify population outliers (>6 standard deviations from the mean after 5 iterations) (80). Following this protocol, 10 subjects were removed from the original dataset of 278 individuals.

Briefly, RNA was extracted from cerebellar tissue using TRIzol® and DNase treated Qiagen RNeasy columns. Libraries were prepared using the Illumina Truseq kit and sequenced on an Illumina Hiseq 2000 instrument to obtain 101bp paired-end reads (3 lanes/sample). Individuals with low mapped reads (<85%) or sex discrepant gene counts (Y-chromosome gene expression) were discarded (20 individuals total). Raw RNA-seq reads were aligned to the

human genome and transcriptome builds GRCh38 and GRCh38.77 respectively using SNAPR; reads were filtered based on Phred scores <= 20 (81). Subsequent BAM files were utilized for determination of alternative allele frequency at the 11 p9 sites using VarScan (82). Gene expression was derived from transcript counts using SNAPR (81); counts were normalized using the trimmed mean of m-values (TMM) method in edgeR while taking into account differences in library size (calcNormFactors)(83).

DETECTION OF MITOCHONDRIAL RNA HETEROPLASMY

Mitochondrial reads were extracted from total RNA-seq BAM files using samtools v.1.34 view (84). For each BAM file, an mpileup file was generated using samtools mpileup. Heteroplasmy was measured at 11 different p9 sites within the mitochondrial transcriptome (585, 1610, 4271, 5520, 7526, 8303, 9999, 10413, 12146, 12274, 14734) from the mpileup files using readcounts in VarScan v.2.4 with default parameters (82). Mitochondrial pseudogenes (NUMTs) were not accounted for, as none of the aforementioned sites have been shown to overlap with NUMT sequences (77). Frequency of alternative alleles were determined for each of the 11 p9 sites based on the Cambridge Reference Sequence (CRS). Degree of post-transcriptional mt-RNA methylation was inferred from alternative allele frequencies using previously published methods (77). A Kolmogorov-Smirnov test determined the data to have a non-normal distribution. Correlation coefficients for p9 methylation across the 11 p9 sites were determined using Spearman Rho. Degree of p9 methylation was compared across disease states using pair-wise Kruskal-Wallis tests with Bonferroni correction for multiple testing at each site (not accounting for the 11 site-based tests).

GENE-BASED GENOME-WIDE ASSOCIATION

Principle component analysis was performed in EIGENSOFT to determine if a considerable amount of heterogeneity was present in the SNP dataset (80). Linkage disequilibrium-based pruning was performed in PLINK (--indep-pairwise 50 5 0.2) yielding a final dataset of 58,174 SNPs (79). Linear association tests adjusting for covariates such as age, sex, eigenvectors 1 to 10 was performed for each p9 site to identify genetic variants associated with methylation (log10 transformed) using the SNP2GENE function of the Functional Mapping and Annotation (FUMA) online platform (85). This tool utilizes MAGMA to map associated SNPs to protein-coding genes (86); mapping window size was conservatively set to 10kb. Genome-wide significance was Bonferroni adjusted to 2.93×10^{-6} based on mapping of input SNPs to 17079 protein-coding genes; Bonferroni correction was applied to each linear association test. Manhattan plots, local regional plots and Q-Q plots to identify genomic inflation in the SNP-set, were generated in FUMA.

GENE EXPRESSION ANALYSIS

Nuclear gene expression correlated with methylation was determined using Spearman's rho. Of note, correlation analysis was restricted to site 585, as the vast majority of sites were tightly correlated with site 585; sites that were not tightly correlated with site 585 (4271 and 14734) did not show significant differences in methylation. The top 1000 transcripts (565 unique genes) and eigenvectors 1 and 2 were visualized using ClustVis (87). Heatmap clustering was based on correlation distance and average linkage with unit variance scaling; clusters were not formally tested for enrichment in regard to disease status. Overrepresentation testing using Fisher's exact test with FDR correction was performed in PANTHER using the top 1000 transcripts (88). Tissue-specific enrichment analysis was conducted using in IPA (Qiagen Inc., https://www.qiagenbioinformatics.com/products/ingenuitypathway-analysis) using the Core Analysis function.

RESULTS

MITOCHONDRIAL POST-TRANSCRIPTIONAL METHYLATION

Degree of post-transcriptional methylation at 11 key sites (585, 1610, 4271, 5520, 7526, 8303, 9999, 10413, 12146, 12274, 14734) throughout the mitochondrial transcriptome was inferred from alternative allele frequencies based on the revised Cambridge reference sequence. Across the 11 p9 sites, variability was observed in the degree of methylation (Figure 7).

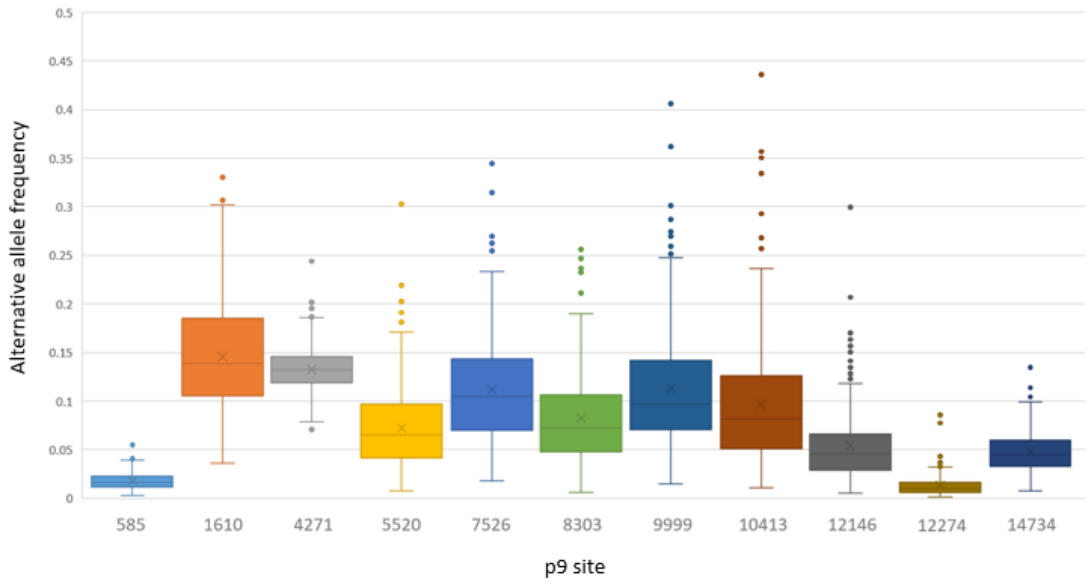

Figure 7. Variation in alternative allele frequency at each of the 11 p9 sites. Alternative allele frequency shown here is cumulative for all individuals (n= 266).

Degree of methylation was also observed to be highly correlated across the 11 p9 sites (Figure 8); specifically, methylation at eight out of the 11 sites appeared to correlate with site 585, with exception of sites 4271 and 14734.

Figure 8. Matrix displaying Spearman rho correlation of methylation across the 11 p9 sites.

For each of the 11 p9 sites, differences in degree of methylation between each of the four groups: normal controls (NC) (n= 74), Alzheimer's disease (AD) (n= 82), progressive supranuclear palsy (PSP) (n= 83) and pathological aging (PA) (n=27) were assessed using non-parametric Kruskal-Wallis pair-wise testing. Significant differences in methylation rate between disease states was observed at a number of p9 sites (Table 4). Interestingly, AD and PSP groups showed similar rates of hypermethylation when compared to NC and PA; no significant differences were seen between NC and PA (Table 4).

Table 4. Summary table displaying methylation distributions and significant group differences per p9 site. Mean ± standard deviation of degree of methylation (inferred from alternative allele frequency) is shown across the top for each site. Non-parametric Kruskal-Wallis p-values with Bonferroni correction (to adjust for multiple comparisons) is shown on the far right. P-values from pair-wise Kruskal-Wallis comparisons between groups are shown within the matrix; p-values<0.05 (*), p-values<0.001 (**).

p9 site		NC	AD	PSP	PA	
585	Mean±SD	0.0140±0.0057	0.0210±0.01067	0.0201±0.0092	0.0142±0.0053	p-value (Bonferroni adj.)
	NC		<0.001	<0.001		<0.001
	AD	**			0.01	
	PSP	**			0.02	
	PA		*	*		
1610		0.1276±0.0456	0.1601±0.0579	0.1546±0.0599	0.1239±0.0339	0.001
	NC		0.003	0.045		
	AD	*			0.018	
	PSP	*			0.1	
	PA		*			
4271		0.1308±0.0247	0.1343±0.0234	0.1304±0.0229	0.1379±0.0239	0.602
	No significant group differences					
5520		0.0610±0.0393	0.0810±0.0409	0.0790±0.0496	0.0576±0.0250	0.002
	NC		0.004	0.072		
	AD	*			0.069	
	PSP				0.357	
	PA					
7526		0.0954±0.0468	0.1217±0.0492	0.1247±0.0685	0.0888±0.0353	0.001
	NC		0.007	0.059		
	AD	*			0.019	
	PSP				0.83	
	PA		*			
8303		0.0687±0.0419	0.0830±0.0455	0.0966±0.0572	0.0758±0.0346	0.01
	NC		0.17	0.006		
	AD					
	PSP	*				
	PA					
9999		0.0929±0.0527	0.1130±0.0546	0.1370±0.0808	0.0921±0.0416	0.001
	NC		0.072	0.001		
	AD				0.518	
	PSP	**			0.055	
	PA					
10413		0.0754±0.04986	0.1000±0.0514	0.1209±0.0857	0.0728±0.0389	<0.001
	NC		0.007	<0.001		
	AD	*			0.131	
	PSP	**			0.031	
	PA			*		
12146		0.0445±0.0278	0.0523±0.0289	0.0658±0.0512	0.0492±0.0232	0.063
	No significant group differences					
12274		0.0103±0.0069	0.0140±0.0086	0.0167±0.0151	0.0099±0.0059	0.004
	NC		0.038	0.024		
	AD	*			0.22	
	PSP	*			0.17	
	PA					
14734		0.0480±0.0211	0.0484±0.0480	0.0474±0.0226	0.0450±0.0178	0.933
	No significant group differences					

GENE-BASED GWAS

Gene-based linear association testing performed in FUMA identified three genes to be significantly associated with p9 methylation. Typed SNPs were mapped to 17079 protein coding genes. Two SNPs (rs12343928; rs4877837) mapped to *SLC28A3* (p-value = 1.935×10^{-6}, CADD score = 24.7) located on chromosome 9, were identified as significantly associated with methylation at site 585 (Figure 9; Appendix 5). Significance of this result was further substantiated by the presence of multiple SNPs in linkage disequilibrium with the lead SNP; as shown in the regional plot (Figure 9). A single SNP (rs2034879) mapped to *SENP8* (CADD score = 13.22)*, MYO9A* (CADD score = 18.35) and *GRAMD2* (CADD score = 16.49) located on chromosome 15 was suggestively associated with methylation at p9 site 585 (Figure 9, Appendix 5); mapping to multiple genes may be due to the conservative ± 10kb window utilized. Lastly, a SNP (rs9872864) mapped to *TRAIP* (p-value = 8.32×10^{-7}, CADD score = 7.558) and nearby gene *IP6K1* (p-value = 6.67×10^{-7}, CADD score = 20.7) located on chromosome 3 was also found to be significantly associated with methylation at six out of the 11 p9 sites (5520, 7526, 8303, 9999, 10413, 12146) (Figure 10; Appendix 5).

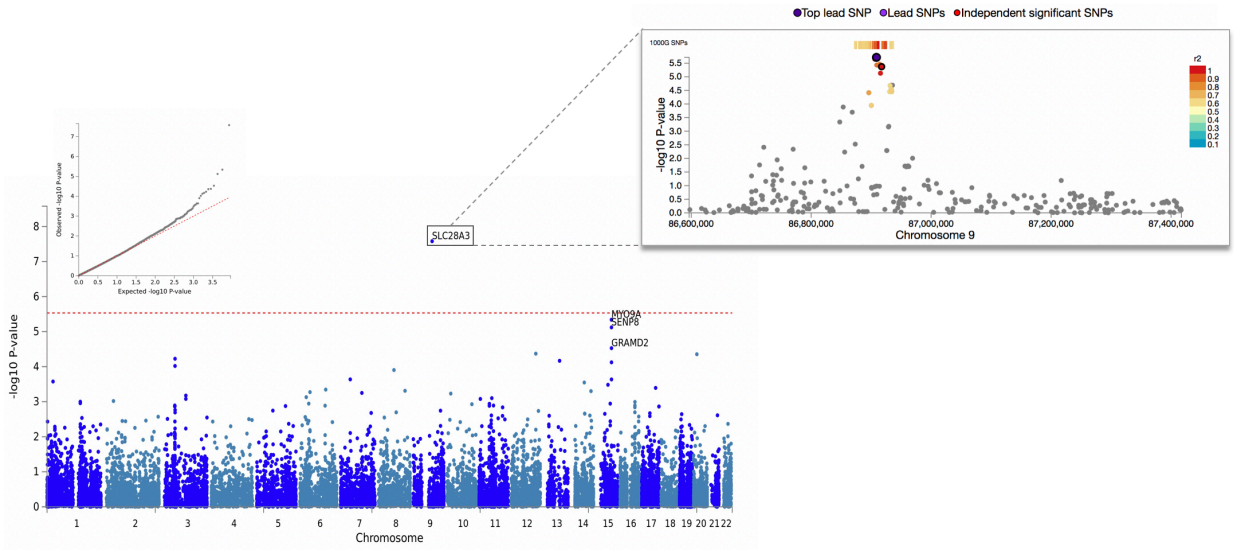

Figure 9. Gene-based associations with degree of methylation at site 585. The Q-Q plot (top left) shows no sign of genomic inflation. The Manhattan plot (bottom left) illustrates a primary signal in *SLC28A3* on chromosome 9 (p-value = 1.935×10^{-6}) and multiple suggestive associations on chromosome 15. The regional plot (top right) displays an 800kb window showing multiple SNPs in LD with the top lead SNP in the gene-based signal.

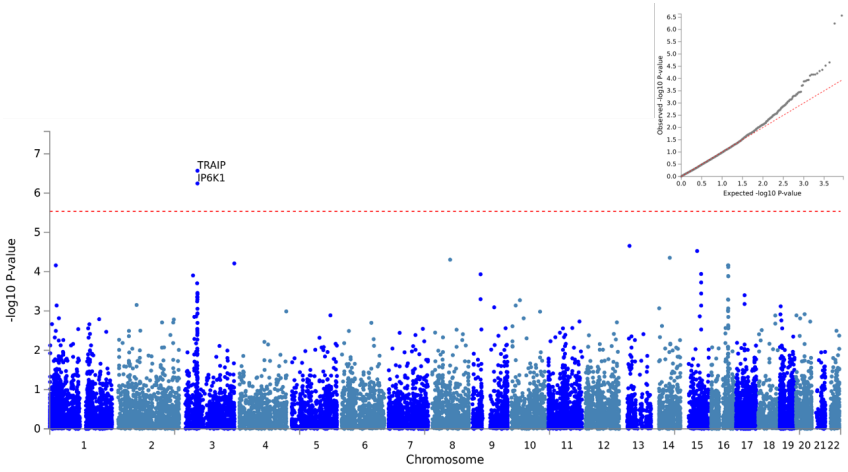

Figure 10. Gene-based associations with degree of methylation at 6 out of 11 sites. The Q-Q plot (top right) shows no sign of genomic inflation. The Manhattan plot (bottom left) illustrates a primary signal in *TRAIP* and *IP6K1* on chromosome 3 (8.32×10^{-7}, 6.67×10^{-7}). This result was replicated in 6 out of 11 p9 sites (results for site 12146 shown here).

MITOCHONDRIAL-RELATED GENE EXPRESSION

The expression of 5300 transcripts was found to be significantly correlated with degree of methylation at site 585. Of note, correlation testing was restricted to methylation at site 585 since 1) significant differences in methylation were observed between disease states at this site and 2) methylation rates at the majority of p9 sites were correlated with site 585. The top 1000 transcripts are visualized in Figure 11. Primary bifurcations demonstrate left and right clades to be enriched for AD/PSP and NC/PA respectively; howver, this enrichment was not formally tested (Figure 11).

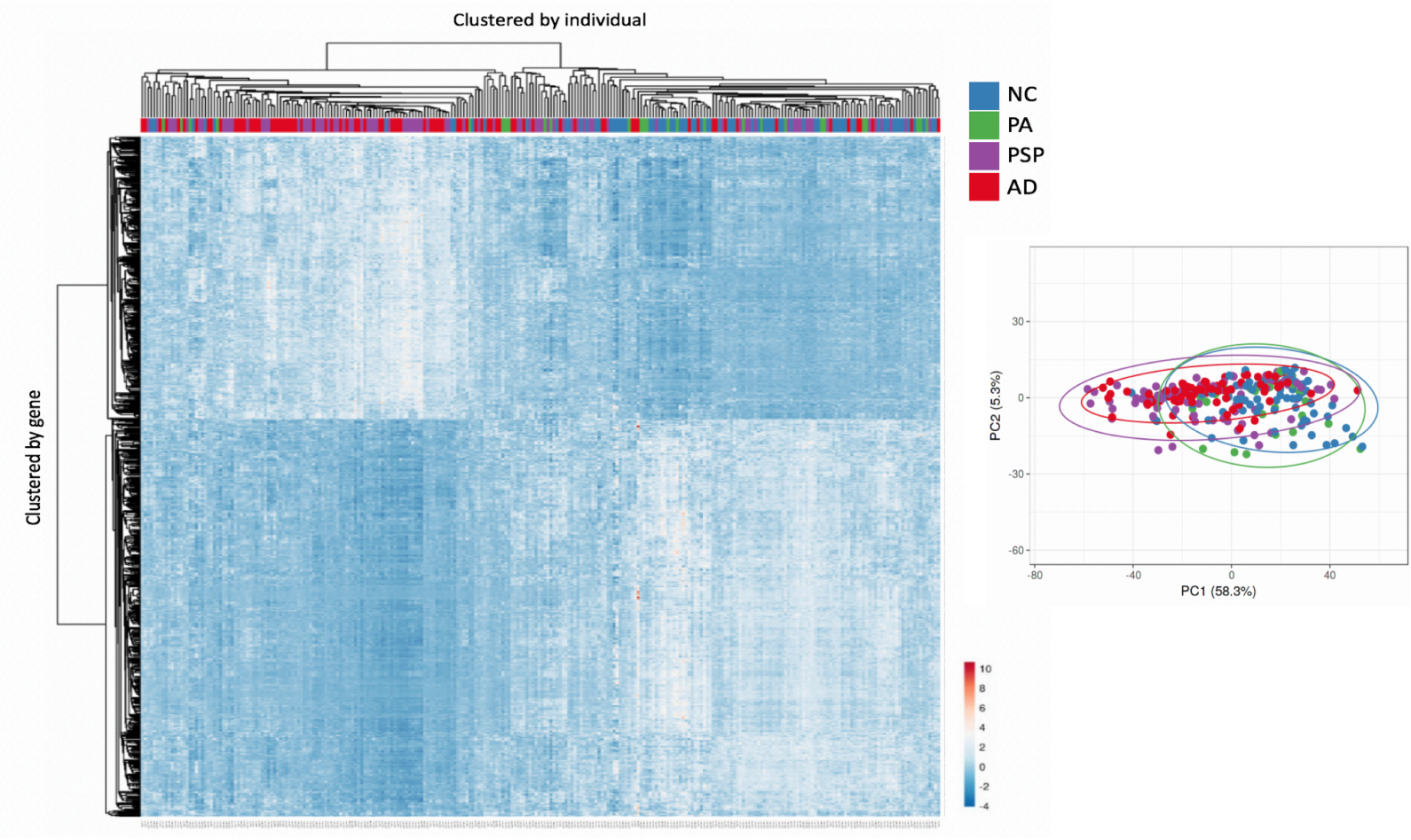

Figure 11. Expression profiles of the top 1000 transcripts significantly associated with degree of p9 methylation at site 585. Heatmap expression profiles are clustered by gene (y-axis) and individual (x-axis) (left). Principle component analysis of gene expression displays overlap between case groups (right). Colors represent disease status; NC (blue), PA (green), AD (red) and PSP (purple) (bottom). Gradient bar represents gene expression level; high expression (red), low expression (blue).

The top 1000 transcripts correlated with methylation rate at p9 site 585 were tested for significantly overrepresented gene ontology categories (e.g. cellular components, molecular functions, biological processes) using PANTHER. A number of GO terms were found to be over-represented in the gene-set including several that were mitochondrially-associated; these are displayed in Figure 12 (Appendix 5).

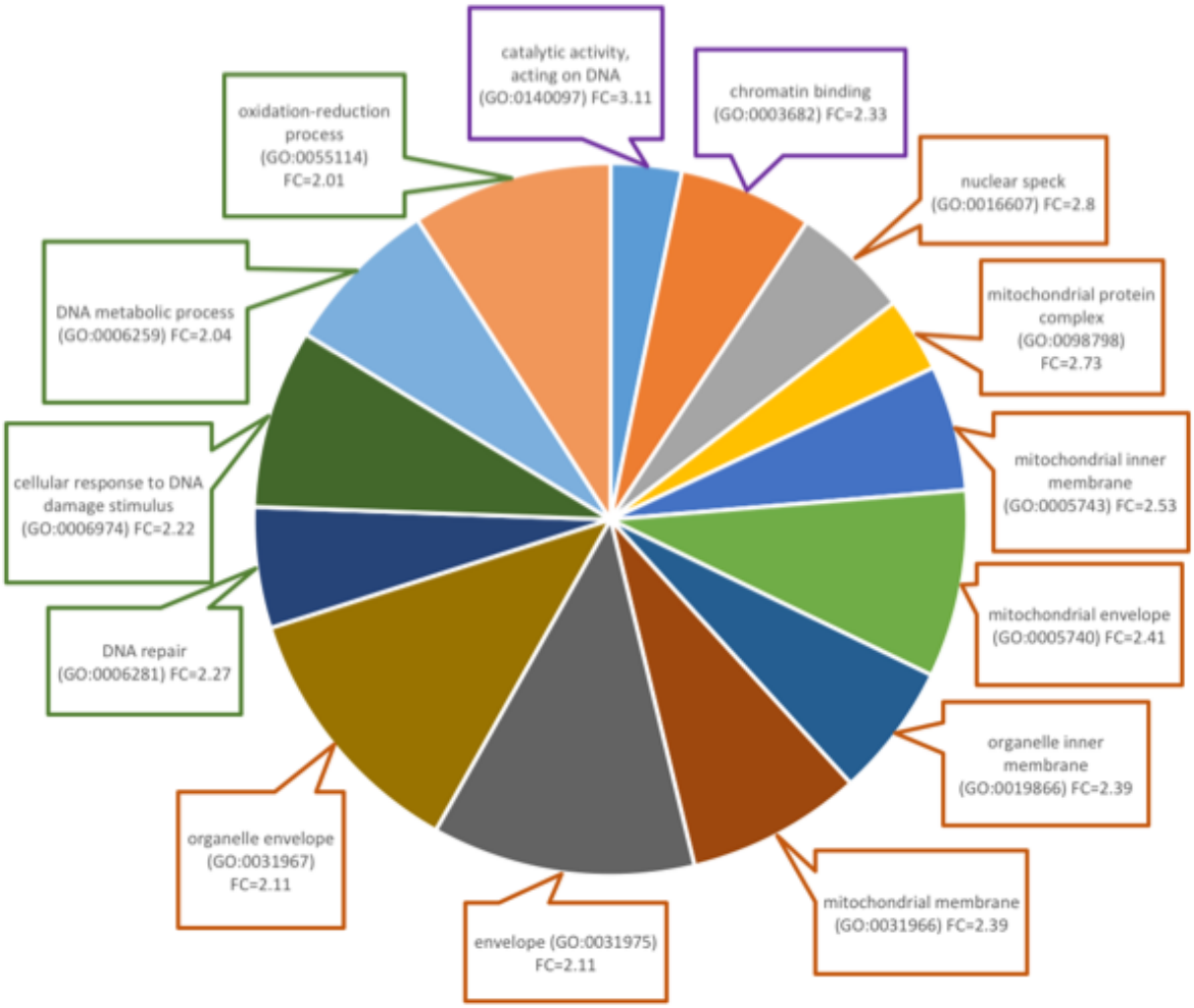

Figure 12. GO terms identified as being overrepresented based on the top 1000 transcripts significantly correlated with p9 methylation at site 585. GO terms are color coded by category; Molecular function (purple), cellular component (orange), biological process (green). Terms were selected using a threshold of >2 fold change. Fold change was determined based on number of enriched genes from our 1000 transcripts list divided by the number of expected enriched genes.

A tissue-specific (i.e. cerebellum) enrichment analysis was then conducted in IPA using all significantly correlated transcripts (5300 unique genes). Several pathways were identified as enriched in our gene-set including many that are linked to mitochondrial function as well as DNA damage/repair (Figure 13; Appendix 5).

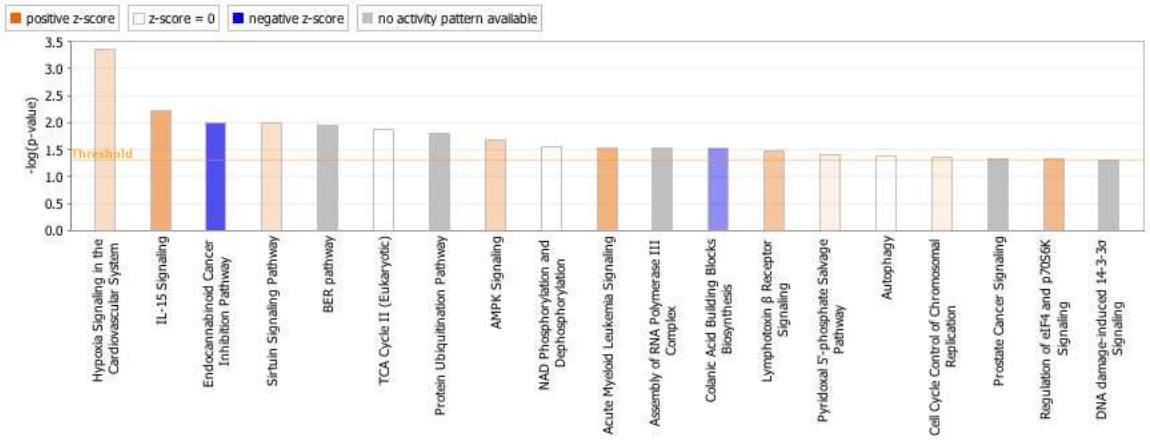

Figure 13. Enriched canonical pathways based on all transcripts significantly correlated with p9 methylation. Pathways positively and negatively correlated with p9 methylation are shown in orange and blue respectively.

DISCUSSION

The presented analysis validates that post-transcriptional methylation occurs consistently at functionally important sites throughout the mitochondrial transcriptome, and this methylation is highly correlated across the 11 multiallelic ("p9") sites. Analyzing RNA sequence data from a clinical-based neuropathological cohort, we observed significant hypermethylation at p9 sites within mt-RNA in the cerebellar tissue of Alzheimer's disease and progressive supranuclear palsy patients. Similarities in post-transcriptional mt-RNA rates may reflect comparable genetic etiologies underlying the cerebellar mitochondrial dysfunction that is a hallmark of both diseases (89, 90). Interestingly, no significant difference in methylation was observed when comparing normal controls to pathological aging. This is unsurprising due to the ambiguity in differentiating normal from pathological aging. Typically, pathological aging is diagnosed based on the presence of brain pathology with lack of phenotypic manifestation (i.e. cognitive decline). It is not uncommon for healthy aged individuals to also display brain pathology, which further obscures our ability to distinguish between healthy and pathological aging (91). Idaghdour and Hodgkinson (2017) also observed hypermethylation of mitochondrial

p9 sites in another age-related disease (i.e. cancer). This supports the idea that p9 hypermethylation may be more closely associated with disease pathology rather than normal aging. However, whether hypermethylation at these sites is a cause or consequence of pathology remains unclear.

Importantly, we must acknowledge the technical limitations associated with traditional RNA-seq workflows such as that used here. In this study, we sought to quantify relative degree of post-transcriptional methylation of mt-tRNAs using total RNA-seq data. Given the small and highly folded nature of mt-tRNAs, they are often difficult to capture. Traditional total RNA sequencing protocols generally do not enrich for and usually detail removal of small RNAs. With this, it is possible that the mature mitochondrial tRNA reads may be under-represented in this dataset and conclusions made here may not be representative of the entire mature mt-tRNA pool. Future studies investigating p9 methylation should utilize small RNA enrichment protocols and perform cDNA size selection prior to RNA sequencing.

NUCLEAR GENES ASSOCIATED WITH P9 METHYLATION

Using gene-based GWAS, we identified several nuclear-encoded genes significantly associated with methylation rate at a number of p9 sites throughout the mitochondrial transcriptome. Two SNPs (rs12343928; rs4877837) mapped to solute carrier family 28 member 3 (*SLC28A3*) located on chromosome 9 were identified as significantly associated with methylation at p9 site 585; a result further substantiated by neighboring SNPs in LD. The protein encoded by *SLC28A3* is involved in regulation of neurotransmission, vascular tone and metabolism of nucleoside drugs; processes that are physiologically relevant to the tissue and disease states studied here. Nucleoside drugs are often used to treat age-related conditions like hypertension and type 2 diabetes (T2D) and is also used to combat mitochondrial dysfunction in Parkinson's disease (PD) (92). This is interesting since PSP bears phenotypic similarities to PD

and both diseases showcase mitochondrial dysfunction as a pathological hallmark. Further, T2D and hypertension are known comorbidities for AD.

A single SNP (rs2034879) mapped to a number of genes (*SENP8, MYO9A, GRAMD2*) on chromosome 15 was identified as suggestively associated with methylation at p9 site 585; the number of mapped genes is likely attributed to the restrictive window size of ±10kb that was used. SENP8 serves as a catalyst in pathways associated with neddylation, a type of post-transcriptional modification similar to ubiquitination. Interestingly, these same pathways are involved in the endocytic degradation of APP and their dysfunction has been observed in AD leading to accumulation of APP and Aβ (93). MYO9A is an unconventional myosin that regulates Rho GTPases within neurons leading to downstream regulation of neuron morphology and function; because of this, Rho GTPases have been investigated as a therapeutic target for neurodegenerative diseases such as AD (94). Specific Rho GTPases have also been implicated in maintenance of mitochondrial homeostasis and apoptotic signaling (95). Though it is not clear, GRAMD2 may play an indirect role in modulating calcium homeostasis through organization of endoplasmic reticulum-plasma membrane contact sites (EPCS) (96). Contact sites between the ER and mitochondria, otherwise termed mitochondrial associated membranes (MAMs) facilitate uptake of calcium from the ER to the mitochondria (97). Importantly, calcium regulates mitochondrial bioenergetics, dynamics and apoptotic signaling; therefore, *GRAMD2* may affect calcium signaling and downstream mitochondrial function.

A single SNP (rs9872864) mapped to *TRAIP* and *IP6K1* on chromosome 3 was identified as significantly associated with methylation at six out of 11 p9 sites (5520, 7526, 8303, 9999, 10413, 12146). TRAIP (TRAF interacting protein) is an E3 ubiquitin ligase involved in cell survival and apoptosis. TRAIP plays an important role at cell cycle checkpoints by regulating spindle assembly, chromosome distribution and DNA damage responses (98). Cell cycle checkpoints serve critical neuroprotective roles; dysregulation of these checkpoints and cell-

cycle re-entry post-mitotic neurons have been previously observed in different tauopathies (99). IP6K1 (inositol hexakisphosphate kinase 1) is responsible for synthesis of 5-diphosphoinositol phentakisphosphate (5-IP_7) from hexakisphosphate (IP_6). IP6K1 serves as an upstream regulator of metabolism (i.e. glucose homeostasis, lipolysis), apoptosis and transcription (100). IP6K1 is known to influence mitochondrial function via regulation of ATP concentration; this is done by altering the ratio of glycolytic to oxidative phosphorylation (101). In knockout (*IP6K1*-/-) yeast models, Szijgyarto et al. observed declines in mitochondrial respiration but paradoxical increases in ATP; this may be explained by elevated glycolysis and depletion of metabolic processes demanding ATP (101). In a disease context, some have investigated IP6K1 as a therapeutic target for obesity and type 2 diabetes (102). Others have identified SNPs within *IP6K1* gene region as associated with AD using tag SNP methods (103). Further, IP6K1 plays a role in lipolysis, a process that is promoted by Aβ accumulation leading to subsequent lipid toxicity and peroxidation resulting in downstream mitochondrial dysfunction (104).

A number of the genes identified here are loosely connected to mitochondrial function, though no loci appear to directly affect mt-tRNA processing. However, the majority (5 of 6) of GWAS identified genes had CADD scores exceeding 10. Briefly, CADD (Combined Annotation Dependent Depletion) scoring is a machine learning approach that allows for estimation of deleteriousness and/or pathogenicity of causal genetic variants; CADD scores >10 are considered to be in the top 10% of deleterious variants within the human genome (105). This may suggest that variants mapped to these five genes may be more closely tied to pathological processes, as opposed to normal aging processes.

In their 2014 publication, Hodgkinson et al. reported several gene associations with p9 methylation—one of which was *MRPP3*, an critical player in mitochondrial tRNA processing (77). The MRPP3 association was not replicated here; though this isn't entirely surprising, as their study was conducted on a cohort of healthy, normal aged adults (40-69 years) with no

obvious signs of pathology, while our study was focused on aged subjects with neuropathology. This may indicate that variability in *MRPP3* associated with p9 methylation (as reported in (77)) is presumably normal, while genetic variability associated with p9 methylation in our study is presumably pathological. These novel genotype associations may be pointing to upstream effectors of overall mitochondrial function. Although, it is important to acknowledge the caveat that all gene-based association tests were performed on all groups combined. This strategy was utilized since the small sample size of each diagnostic category (NC, AD, PSP, PA) left us underpowered to detect significant associations when analyzing each group separately. Provided that we observed p9 hypermethylation in both AD and PSP, it is possible that significant gene associations may be driven by individual pathologies and not necessarily post-transcriptional RNA processes.

MITOCHONDRIAL-RELATED NUCLEAR GENE EXPRESSION CORRELATED WITH P9 METHYLATION

Here we identified 5300 genes significantly correlated with p9 methylation. Using principle component analysis, gene expression profiles appeared to cluster by disease state with AD and PSP, and NC and PA grouping together respectively. Of the top gene expression hits, several GO terms related to a number of cellular components and processes were identified as overrepresented using PANTHER. Of interest was the enrichment for mitochondrial components. Other GO terms such as *DNA repair and cellular response to DNA damage stimulus*, appeared to correlate with one of the top genes (i.e.*TRAIP*) that was identified in the gene-based GWAS. Though some of the GO terms are ambiguous, these findings do suggest that p9 methylation is associated with altered transcription of gene-sets critical for mitochondrial function.

In order to identify tissue-specific changes, we performed further enrichment analysis in IPA using a cerebellum tissue reference and all of the transcripts (5300 unique genes) significantly correlated with p9 methylation. Again, several of the enriched pathways identified were linked to mitochondrial function and homeostasis, as well as DNA damage/repair. We also identified a number of pathways related to RNA processing. In addition, some of the GO terms (e.g. DNA repair and cellular response to DNA damage stimulus) and canonical pathways (e.g. Cell cycle control of chromosomal replication, DNA damage induced 14-3-3σ signaling) appeared to correlate with functions of one of the top genes (i.e.*TRAIP*) identified in the gene-based GWAS. Though some of the GO terms and canonical pathways are rather ambiguous, it does imply that p9 methylation is associated with altered transcription of gene-sets important for mitochondrial function.

CONCLUSION

This is the first work analyzing mitochondrial p9 methylation in the context of neurodegeneration. Here we report an association between p9 methylation and nuclear-encoded gene expression, as well as mitochondrial-related regulation; although, the implications of these associations are unclear. We observed post-transcriptional mt-tRNA hypermethylation and nuclear gene expression profiles in the cerebellum of Alzheimer's disease and progressive supranuclear palsy patients. Although technical limitations in this analysis do not allow us to conclude on methylation status of the mature tRNA pool, the results here are likely indicative of molecular similarities underlying the mitochondrial dysfunction already known to occur within the cerebellum of individuals diagnosed with either of these tauopathies.

A basal level of p9 methylation is required for proper tRNA folding and stability (73) and the degree of methylation at p9 sites has been shown by other groups to have low inter-individual variability (106). In addition, p9 hypermethylation has been observed in other age-

related diseases such as cancer (78). We propose that p9 hypermethylation in AD and PSP may be more closely associated with pathology as opposed to normal aging. We observed that specific nuclear encoded variants increase risk for hypermethylation at mitochondrial p9 sites within cerebellar neurons, but importantly, causality is still not clear (i.e. associations may be linked to pathological processes and not necessarily RNA methylation). For example, hypermethylation of p9 may be the primary event that impacts the function of the ETC and results in mitochondrial dysfunction, due to the influence that p9 methylation has on downstream mitochondrial protein translation (Figure 14). Alternatively, it is possible that ETC dysfunction is the primary event that causes altered p9 methylation, in which case, the p9 hypermethylation is serving as an endophenotype of genetic risk for mitochondrial dysfunction. Regardless, through retrograde signaling, mitochondrial dysfunction may impact nuclear gene expression resulting in alterations in cellular and molecular processes to further exacerbate neurodegenerative pathology.

Though at present, it is unclear whether mt-tRNA methylation is a cause or consequence of pathology, these results point to a potential role for mitochondrial post-transcriptional methylation in the pathophysiology of common tauopathies such as Alzheimer's disease and progressive supranuclear palsy. Given this, post-transcriptional mt-tRNA methylation may serve as an exciting area of investigation for the development of future treatment strategies for neurodegenerative disease.

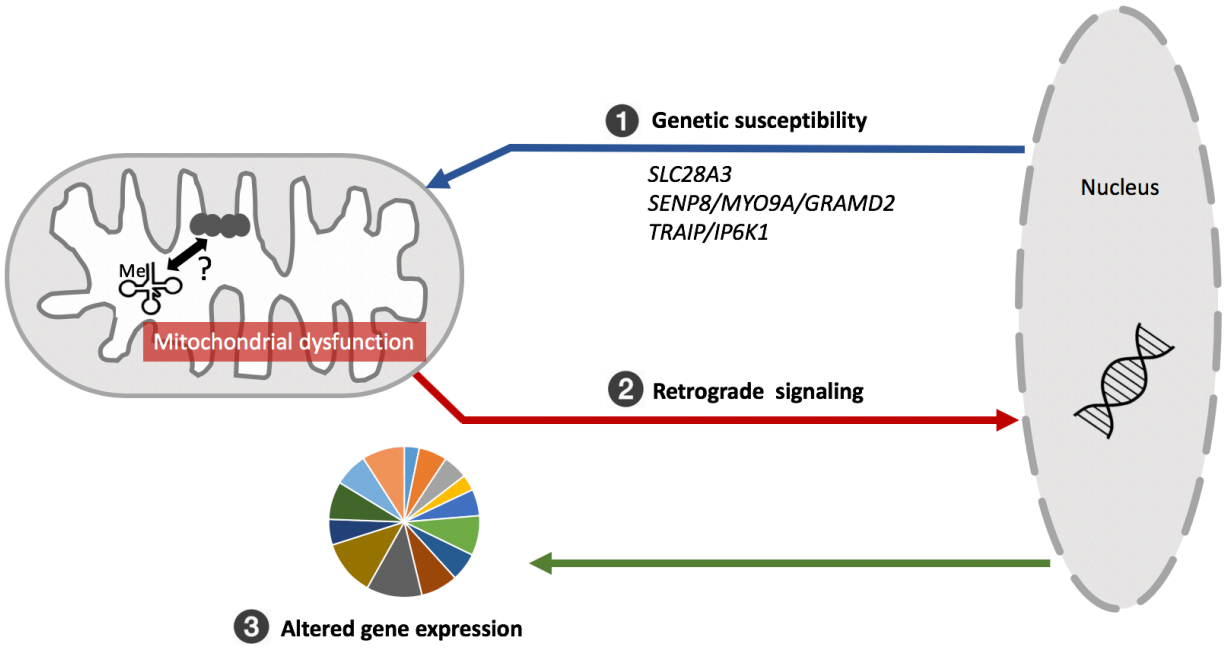

Figure 14. Hypothetical schematic of potential causes and effects of p9 methylation in neurodegeneration. (1) Nuclear encoded genetic variants may be causal for p9 hypermethylation within neuronal mitochondria, resulting in onset or exacerbation of electron transport chain dysfunction. (2) Subsequent mitochondrial dysfunction may lead to altered downstream nuclear gene expression via retrograde signaling resulting in (3) changes to various molecular and cellular processes that further contribute to neurodegenerative pathology.

ACKNOWLEDGEMENTS

Study data were provided by the following sources: The Mayo Clinic Alzheimer's Disease Genetic Studies, led by Dr. Nilufer Taner and Dr. Steven G. Younkin, Mayo Clinic, Jacksonville, FL using samples from the Mayo Clinic Study of Aging, the Mayo Clinic Alzheimer's Disease Research Center, and the Mayo Clinic Brain Bank. Data collection was supported through funding by NIA grants P50 AG016574, R01 AG032990, U01 AG046139, R01 AG018023, U01 AG006576, U01 AG006786, R01 AG025711, R01 AG017216, R01 AG003949, NINDS grant R01 NS080820, CurePSP Foundation, and support from Mayo Foundation. Study data includes samples collected through the Sun Health Research Institute Brain and Body Donation Program of Sun City, Arizona. The Brain and Body Donation Program is supported by the National

Institute of Neurological Disorders and Stroke (U24 NS072026 National Brain and Tissue Resource for Parkinson's Disease and Related Disorders), the National Institute on Aging (P30 AG19610 Arizona Alzheimer's Disease Core Center), the Arizona Department of Health Services (contract 211002, Arizona Alzheimer's Research Center), the Arizona Biomedical Research Commission (contracts 4001, 0011, 05-901 and 1001 to the Arizona Parkinson's Disease Consortium) and the Michael J. Fox Foundation for Parkinson's Research.

Chapter III Noteworthy Results

- Mitochondrial p9 sites are hypermethylated in Alzheimer's disease and progressive supranuclear palsy patients
- Nuclear-encoded genes may confer risk for p9 hypermethylation
- Hypermethylation at mitochondrial p9 sites may be a cause or consequence of altered cellular processes resulting in mitochondrial dysfunction

CHAPTER IV: DISCUSSION

In-depth investigations of the transcriptome in the context of aging and complex disease have grown in number over recent decades. Though RNA is only an intermediate within the central dogma schema, it presents as a valuable resource for understanding the functional molecular significance of genetic variability and epigenetic alterations and the subsequent biological changes that underly specific conditions. With respect to AD, changes to gene expression or transcriptomic epigenetic modifications such as those investigated here, may be informative of molecular pathophysiology; however, whether these molecular-level changes are a cause or consequence of cognitive impairment pathology remains unclear and is an area requiring further investigation.

CONNECTING TRANSCRIPTOMIC SIGNATURES OF COGNITIVE IMPAIRMENT PHENOTYPES

The aforementioned chapters examined the transcriptional and post-transcriptional changes that underly cognitive impairment in its varying forms. The first study investigated differential gene expression signatures in peripheral blood of cognitively impaired Mexican Americans. We identified several genes to be differentially expressed, many of which point to inflammation, cell development, differentiation and death, chromatin regulation/epigenetic modifications and RNA processing underlying the pathophysiology of MCI, a known precursor condition to Alzheimer's-related dementia. Interestingly, the implicated biological processes overlap with known pathophysiological hallmarks of AD. In the second study, we observed post-transcriptional hypermethylation at key sites (i.e. p9 sites) within the mitochondrial transcriptome in post-mortem cerebellar tissue of Caucasians diagnosed with AD and PSP. This hypermethylation was found to be associated with nuclear-encoded genetic variants and

correlated with expression of a number of nuclear-encoded genes that were enriched for a variety of processes including mitochondrial homeostasis, DNA repair, chromatin binding and autophagy.

Each study presented here provides a unique glimpse into the pathophysiology of cognitive impairment. There is an interesting overlap between some of the enriched processes implicated in the two datasets, however, attempts to draw connections between the two studies is complicated due to the distinct methodologies that were utilized. It is important to acknowledge that each study made use of different biological tissues (peripheral blood vs. brain). Since AD-related pathology is mostly brain focused, with specific regions (i.e. hippocampus) being more severely affected in earlier stages of the disease, it would seem logical to study biological changes occurring within brain tissue. However, an obvious caveat to using brain tissue is that it is post-mortem. Molecular signatures within post-mortem tissues are informative, although this sample type does not allow for examination of longitudinal changes in pathology. Studies of peripheral blood—though not a direct measure of biological alterations occurring within the brain—are useful in their own right as they provide insight into systemic changes associated with AD pathology and allow for investigations of living subjects. In this case, use of peripheral blood samples allowed for us to investigate individuals suffering from a condition known to precede AD (i.e. MCI). Given that molecular markers in peripheral blood have been shown to be highly correlated with brain pathology (70), assessments in the periphery of this nature may be of prognostic value.

The studies also investigated varying forms of cognitive impairment in individuals of different ancestral backgrounds (Mexican American vs. Caucasian). Though some aspects of AD pathology will inevitably be similar in all individuals regardless of ancestry, there is evidence to suggest that certain racial/ethnic groups experience distinct types of AD-related cognitive impairment (70). Further, observations of AD-related changes in mild cognitively impaired

individuals such as those seen here, may support the notion that cognition is a spectrum. Following this view, cognitive impairment may present as dynamic and continuous, rather than discrete phenotypes. It is possible that the changes observed in peripheral blood of MCI participants may be early signs of impairment and these same changes may be exacerbated in later stages of cognitive impairment (i.e. AD) pathophysiology.

In both studies, we identified enrichment for processes related to chromatin binding, remodeling and epigenetic modifications. Epigenetic modifications have a well-documented role in AD. Though these changes are often context-specific, our observations are consistent with what has previously been reported in cognitive impairment. In particular, chromatin remodeling and histone modifications including acetylation and methylation have been implicated in AD; for a recent review of epigenetic modifications in neurodegenerative disease, refer to (107). We also observed enrichment for DNA damage response in both datasets; accumulation of DNA damage and altered responses have been extensively studied in the context of AD (108). Further, we identified overlapping enrichment for processes related to protein degradation and cell death. Both the endolysosomal and protein ubiquitin systems serve to regulate protein homeostasis through degradation of damaged or misfolded proteins. In the context of AD, dysfunction of both of these systems has been reported by several groups (109). Lastly, mitochondrial dysfunction is a known hallmark of AD pathology. Though we only identified indirect links to mitochondrial function in our differential gene expression study (i.e. cardiolipin synthesis), the second study investigating post-transcriptional mt-tRNA methylation demonstrated clear links between cognitive impairment pathology and mitochondrial function. We speculate that the lack of mitochondrial-related findings in MCI may be pointing to mitochondrial dysfunction as a hallmark of later stages of disease pathophysiology.

SCIENTIFIC IMPACT

The transcriptome provides a plethora of functionally relevant information. The findings presented here have the potential to progress the field of AD research for several reasons. To begin, the AD literature for Mexican Americans is scant. Here we provided the first study exploring differentially expressed genes in peripheral blood of cognitively impaired Mexican Americans. It has become clear that the associated risk factors and pathophysiology of cognitive impairment experienced by Mexican Americans differs substantially from what has previously been observed in NHWs. Our study provides insight into the molecular changes underlying cognitive impairment in this sub-population. Further, both mitochondrial dysfunction and epigenetic alterations have been implicated in cognitive impairment. However, no groups have investigated the intersection of these two things. Here we detail the first investigation of mt-tRNA methylation in the context of cognitive impairment phenotypes. This study provided a more detailed view into the complexities behind mitochondrial dysfunction. Importantly, the overlapping processes and pathways implicated in both studies may be pointing to early hallmarks of cognitive impairment pathology that are detectable in the periphery. This opens up additional avenues of research investigating the timing of these molecular malfunctions over the progression of the disease. Future studies will be focused on replication of results (due to the small sample sizes used here) and follow-up of these molecular signatures throughout progression of AD using longitudinal samples.

REFERENCES

1. Mather M, P. Scommegna, L. Kilduff. Fact Sheet: Aging in the United States Population Reference Bureau2019 [
2. 2019 Alzheimer's disease facts and figures. Alzheimer's & Dementia. 2019;15(3):321-87.
3. Du X, Wang X, Geng M. Alzheimer's disease hypothesis and related therapies. Transl Neurodegener. 2018;7:2-.
4. Chinnery PF, Hudson G. Mitochondrial genetics. British Medical Bulletin. 2013;106(1):135-59.
5. William F. Martin MM. The Origin of Mitochondria. Nature Education. 2010;3(59):58.
6. Gray MW, Burger G, Lang BF. Mitochondrial Evolution. Science. 1999;283(5407):1476-81.
7. Wang Y, Brinton RD. Triad of risk for late onset Alzheimer's: Mitochondrial haplotype, APOE genotype and chromosomal sex. Frontiers in aging neuroscience. 2016;8.
8. Wallace DC, Brown MD, Lott MT. Mitochondrial DNA variation in human evolution and disease. Gene. 1999;238(1):211-30.
9. Holt IJ, Reyes A. Human Mitochondrial DNA Replication. Cold Spring Harbor Perspectives in Biology. 2012;4(12):a012971.
10. Swerdlow RH, Koppel S, Weidling I, Hayley C, Ji Y, Wilkins HM. Mitochondria, Cybrids, Aging, and Alzheimer's Disease. Prog Mol Biol Transl Sci. 2017;146:259-302.
11. Johri A, Beal MF. Mitochondrial Dysfunction in Neurodegenerative Diseases. Journal of Pharmacology and Experimental Therapeutics. 2012;342(3):619-30.
12. Swerdlow RH, Burns JM, Khan SM. The Alzheimer's disease mitochondrial cascade hypothesis: progress and perspectives. Biochimica et Biophysica Acta (BBA)-Molecular Basis of Disease. 2014;1842(8):1219-31.
13. Albrekkan FM, Kelly-Worden M. Mitochondrial Dysfunction and Alzheimer°Øs Disease. Open Journal of Endocrine and Metabolic Diseases. 2013;Vol.03No.02:6.
14. Gatz M, Pedersen NL, Berg S, Johansson B, Johansson K, Mortimer JA, et al. Heritability for Alzheimer's Disease: The Study of Dementia in Swedish Twins. The Journals of Gerontology: Series A. 1997;52A(2):M117-M25.
15. Cuyvers E, Sleegers K. Genetic variations underlying Alzheimer's disease: evidence from genome-wide association studies and beyond. The Lancet Neurology. 2016;15(8):857-68.
16. Barber RC. The genetics of Alzheimer's disease. Scientifica (Cairo). 2012;2012:246210-.
17. Tang M, Stern Y, Marder K, et al. The apoe-∈4 allele and the risk of alzheimer disease among african americans, whites, and hispanics. JAMA. 1998;279(10):751-5.
18. Silzer T, Barber R, Sun J, Pathak G, Johnson L, O'Bryant S, et al. Circulating mitochondrial DNA: New indices of type 2 diabetes-related cognitive impairment in Mexican Americans. PLOS ONE. 2019;14(3):e0213527.
19. Phillips N, Barber R, Roby R. Longitudinal assessment of mitochondrial DNA copy number and deletion ratio in peripheral blood of people with Alzheimer's: A Texas Alzheimer's Research and Care Consortium Project. Alzheimer's & Dementia. 2013;9(4, Supplement):P206.
20. Centers for Disease Control and Prevention. National Diabetes Statistics Report A, GA: Centers for Disease Control and Prevention, U.S. Dept of Health and Human Services; 2017.
21. Zilliox LA, Chadrasekaran K, Kwan JY, Russell JW. Diabetes and cognitive impairment. Current diabetes reports. 2016;16(9):87.

22. Martorell R. Diabetes and Mexicans: why the two are linked. Preventing chronic disease. 2005;2(1).
23. Silzer TK, Phillips, N.R. Etiology of type 2 diabetes and Alzheimer's disease: Exploring the

mitochondria. Mitochondrion. 2018.
24. Karahalil B. Overview of Systems Biology and Omics Technologies. Current medicinal chemistry. 2016;23(37):4221-30.
25. Han Y, Gao S, Muegge K, Zhang W, Zhou B. Advanced Applications of RNA Sequencing and Challenges. Bioinform Biol Insights. 2015;9(Suppl 1):29-46.
26. L. Noe-Bustamante FAaSS. Facts on Hispanics of Mexican origin in the United States, 2017: Pews Research Center 2019 [Available from: https://www.pewresearch.org/hispanic/fact-sheet/u-s-hispanics-facts-on-mexican-origin-latinos/.
27. O'Bryant SE, Johnson L, Balldin V, Edwards M, Barber R, Williams B, et al. Characterization of Mexican Americans with mild cognitive impairment and Alzheimer's disease. Journal of Alzheimer's disease : JAD. 2013;33(2):373-9.
28. Haan MN, Mungas DM, Gonzalez HM, Ortiz TA, Acharya A, Jagust WJ. Prevalence of Dementia in Older Latinos: The Influence of Type 2 Diabetes Mellitus, Stroke and Genetic Factors. Journal of the American Geriatrics Society. 2003;51(2):169-77.
29. O'Bryant SE, Humphreys JD, Schiffer RB, Sutker PB. Presentation of Mexican Americans to a memory disorder clinic. Journal of Psychopathology and Behavioral Assessment. 2007;29(3):137.
30. Hampel H, O'Bryant SE, Molinuevo JL, Zetterberg H, Masters CL, Lista S, et al. Blood-based biomarkers for Alzheimer disease: mapping the road to the clinic. Nat Rev Neurol. 2018;14(11):639-52.
31. O'Bryant SE, Xiao G, Barber R, Reisch J, Doody R, Fairchild T, et al. A Serum Protein–Based Algorithm for the Detection of Alzheimer Disease. Archives of Neurology. 2010;67(9):1077-81.
32. Pathak GA, Silzer TK, Sun J, Zhou Z, Daniel AA, Johnson L, et al. Genome-Wide Methylation of Mild Cognitive Impairment in Mexican Americans Highlights Genes Involved in Synaptic Transport, Alzheimer's Disease-Precursor Phenotypes, and Metabolic Morbidities. Journal of Alzheimer's Disease. 2019;72:733-49.
33. Andrews S. FastQC: a quality control tool for high throughput sequence data. Babraham Bioinformatics, Babraham Institute, Cambridge, United Kingdom; 2010.
34. Love MI, Huber W, Anders S. Moderated estimation of fold change and dispersion for RNA-seq data with DESeq2. Genome Biol. 2014;15(12):550-.
35. Gallego Romero I, Pai AA, Tung J, Gilad Y. RNA-seq: impact of RNA degradation on transcript quantification. BMC Biology. 2014;12(1):42.
36. Durinck S, Spellman PT, Birney E, Huber W. Mapping identifiers for the integration of genomic datasets with the R/Bioconductor package biomaRt. Nat Protoc. 2009;4(8):1184-91.
37. Ge SX, Jung D, Yao R. ShinyGO: a graphical gene-set enrichment tool for animals and plants. Bioinformatics. 2019.
38. Szklarczyk D, Gable AL, Lyon D, Junge A, Wyder S, Huerta-Cepas J, et al. STRING v11: protein–protein association networks with increased coverage, supporting functional discovery in genome-wide experimental datasets. Nucleic Acids Research. 2018;47(D1):D607-D13.

39. Vega IE, Cabrera LY, Wygant CM, Velez-Ortiz D, Counts SE. Alzheimer's Disease in the Latino Community: Intersection of Genetics and Social Determinants of Health. J Alzheimers Dis. 2017;58(4):979-92.
40. Doehner J, Knuesel I. Reelin-mediated Signaling during Normal and Pathological Forms of Aging. Aging Dis. 2010;1(1):12-29.
41. Mosher KI, Wyss-Coray T. Microglial dysfunction in brain aging and Alzheimer's disease. Biochemical Pharmacology. 2014;88(4):594-604.
42. Zhang B, Gaiteri C, Bodea L-G, Wang Z, McElwee J, Podtelezhnikov AA, et al. Integrated systems approach identifies genetic nodes and networks in late-onset Alzheimer's disease. Cell. 2013;153(3):707-20.
43. Lim SL, Tran DN, Zumkehr J, Chen C, Ghiaar S, Kieu Z, et al. Inhibition of hematopoietic cell kinase dysregulates microglial function and accelerates early stage Alzheimer's disease-like neuropathology. Glia. 2018;66(12):2700-18.
44. Götzl JK, Brendel M, Werner G, Parhizkar S, Sebastian Monasor L, Kleinberger G, et al. Opposite microglial activation stages upon loss of PGRN or TREM2 result in reduced cerebral glucose metabolism. EMBO Mol Med. 2019;11(6).
45. Itoh Y, Voskuhl RR. Cell specificity dictates similarities in gene expression in multiple sclerosis, Parkinson's disease, and Alzheimer's disease. PLOS ONE. 2017;12(7):e0181349.
46. Thome AD, Faridar A, Beers DR, Thonhoff JR, Zhao W, Wen S, et al. Functional alterations of myeloid cells during the course of Alzheimer's disease. Molecular Neurodegeneration. 2018;13(1):61.
47. Blunsom NJ, Cockcroft S. CDP-Diacylglycerol Synthases (CDS): Gateway to Phosphatidylinositol and Cardiolipin Synthesis. Front Cell Dev Biol. 2020;8:63-.
48. Wood PL, Medicherla S, Sheikh N, Terry B, Phillipps A, Kaye JA, et al. Targeted Lipidomics of Fontal Cortex and Plasma Diacylglycerols (DAG) in Mild Cognitive Impairment and Alzheimer's Disease: Validation of DAG Accumulation Early in the Pathophysiology of Alzheimer's Disease. Journal of Alzheimer's disease : JAD. 2015;48(2):537-46.
49. Kao Y-C, Ho P-C, Tu Y-K, Jou IM, Tsai K-J. Lipids and Alzheimer's Disease. Int J Mol Sci. 2020;21(4):1505.
50. Paradies G, Paradies V, Ruggiero FM, Petrosillo G. Role of Cardiolipin in Mitochondrial Function and Dynamics in Health and Disease: Molecular and Pharmacological Aspects. Cells. 2019;8(7):728.
51. Wood PL PA, Woltjer RL, Kaye JA, Quinn JF. Increased Lysophosphatidylethanolamine and Diacylglycerol levels in Alzheimer's Disease Plasma. JSM Alzheimer's Dis Related Dementia 2014;1(1).
52. Kumar R, Cheok CF. RIF1: A novel regulatory factor for DNA replication and DNA damage response signaling. DNA Repair. 2014;15:54-9.
53. Cornacchia D, Dileep V, Quivy J-P, Foti R, Tili F, Santarella-Mellwig R, et al. Mouse Rif1 is a key regulator of the replication-timing programme in mammalian cells. The EMBO Journal. 2012;31(18):3678-90.
54. Park SY, Seo J, Chun Y-S. Targeted Downregulation of kdm4a Ameliorates Tau-engendered Defects in Drosophila melanogaster. J Korean Med Sci. 2019;34(33).
55. Lee T, Lee H. Prediction of Alzheimer's disease using blood gene expression data. Scientific Reports. 2020;10(1):3485.

56. Rahman MR, Islam T, Shahjaman M, Quinn JMW, Holsinger RMD, Moni MA. Identification of common molecular biomarker signatures in blood and brain of Alzheimer's disease. bioRxiv. 2019:482828.
57. Luco RF, Pan Q, Tominaga K, Blencowe BJ, Pereira-Smith OM, Misteli T. Regulation of Alternative Splicing by Histone Modifications. Science. 2010;327(5968):996-1000.
58. Wei C-J, Cui P, Li H, Lang W-J, Liu G-Y, Ma X-F. Shared genes between Alzheimer's disease and ischemic stroke. CNS Neurosci Ther. 2019;25(8):855-64.
59. Yonekawa T, Thorburn A. Autophagy and cell death. Essays in biochemistry. 2013;55:105-17.
60. Piras A, Collin L, Grüninger F, Graff C, Rönnbäck A. Autophagic and lysosomal defects in human tauopathies: analysis of post-mortem brain from patients with familial Alzheimer disease, corticobasal degeneration and progressive supranuclear palsy. Acta neuropathologica communications. 2016;4:22.
61. Nixon RA, Wegiel J, Kumar A, Yu WH, Peterhoff C, Cataldo A, et al. Extensive Involvement of Autophagy in Alzheimer Disease: An Immuno-Electron Microscopy Study. Journal of Neuropathology & Experimental Neurology. 2005;64(2):113-22.
62. François A, Julian A, Ragot S, Dugast E, Blanchard L, Brishoual S, et al. Inflammatory Stress on Autophagy in Peripheral Blood Mononuclear Cells from Patients with Alzheimer's Disease during 24 Months of Follow-Up. PloS one. 2015;10(9):e0138326-e.
63. Jin K, Peel AL, Mao XO, Xie L, Cottrell BA, Henshall DC, et al. Increased hippocampal neurogenesis in Alzheimer's disease. Proceedings of the National Academy of Sciences. 2004;101(1):343-7.
64. Hohsfield LA, Humpel C. Migration of blood cells to β-amyloid plaques in Alzheimer's disease. Experimental Gerontology. 2015;65:8-15.
65. Rao MV, Mohan PS, Peterhoff CM, Yang D-S, Schmidt SD, Stavrides PH, et al. Marked calpastatin (CAST) depletion in Alzheimer's disease accelerates cytoskeleton disruption and neurodegeneration: neuroprotection by CAST overexpression. J Neurosci. 2008;28(47):12241-54.
66. Ferreira A. Calpain dysregulation in Alzheimer's disease. ISRN Biochem. 2012;2012:728571-.
67. Caramelli P, Nitrini R, Maranhão R, Lourenço ACG, Damasceno MC, Vinagre C, et al. Increased apolipoprotein B serum concentration in Alzheimer's disease. Acta Neurologica Scandinavica. 1999;100(1):61-3.
68. Song F, Poljak A, Crawford J, Kochan NA, Wen W, Cameron B, et al. Plasma Apolipoprotein Levels Are Associated with Cognitive Status and Decline in a Community Cohort of Older Individuals. PLOS ONE. 2012;7(6):e34078.
69. Tang R, Liu H. Identification of Temporal Characteristic Networks of Peripheral Blood Changes in Alzheimer's Disease Based on Weighted Gene Co-expression Network Analysis. Frontiers in Aging Neuroscience. 2019;11(83).
70. O'Bryant SE, Xiao G, Edwards M, Devous M, Gupta VB, Martins R, et al. Biomarkers of Alzheimer's Disease Among Mexican Americans. Journal of Alzheimer's disease : JAD. 2013;34(4):841-9.
71. Duechler M, Leszczyńska G, Sochacka E, Nawrot B. Nucleoside modifications in the regulation of gene expression: focus on tRNA. Cell Mol Life Sci. 2016;73(16):3075-95.

72. Voigts-Hoffmann F, Hengesbach M, Kobitski AY, van Aerschot A, Herdewijn P, Nienhaus GU, et al. A Methyl Group Controls Conformational Equilibrium in Human Mitochondrial tRNALys. Journal of the American Chemical Society. 2007;129(44):13382-3.
73. Helm M, Giegé R, Florentz C. A Watson−Crick Base-Pair-Disrupting Methyl Group (m1A9) Is Sufficient for Cloverleaf Folding of Human Mitochondrial tRNALys Biochemistry. 1999;38(40):13338-46.
74. Zhang C, Jia G. Reversible RNA Modification N(1)-methyladenosine (m(1)A) in mRNA and tRNA. Genomics Proteomics Bioinformatics. 2018;16(3):155-61.
75. Bohnsack MT, Sloan KE. The mitochondrial epitranscriptome: the roles of RNA modifications in mitochondrial translation and human disease. Cellular and Molecular Life Sciences. 2018;75(2):241-60.
76. Lopez Sanchez MIG, Mercer TR, Davies SMK, Shearwood A-MJ, Nygård KKA, Richman TR, et al. RNA processing in human mitochondria. Cell Cycle. 2011;10(17):2904-16.
77. Hodgkinson A, Idaghdour Y, Gbeha E, Grenier J-C, Hip-Ki E, Bruat V, et al. High-Resolution Genomic Analysis of Human Mitochondrial RNA Sequence Variation. Science. 2014;344(6182):413-5.
78. Idaghdour Y, Hodgkinson A. Integrated genomic analysis of mitochondrial RNA processing in human cancers. Genome medicine. 2017;9(1):36-.
79. Purcell S, Neale B, Todd-Brown K, Thomas L, Ferreira Manuel A R, Bender D, et al. PLINK: A Tool Set for Whole-Genome Association and Population-Based Linkage Analyses. American Journal of Human Genetics. 2007;81(3):559-75.
80. Patterson N, Price AL, Reich D. Population Structure and Eigenanalysis. PLOS Genetics. 2006;2(12):e190.
81. Magis AT, Funk CC, Price ND. SNAPR: a bioinformatics pipeline for efficient and accurate RNA-seq alignment and analysis. IEEE Life Sci Lett. 2015;1(2):22-5.
82. Koboldt DC, Chen K, Wylie T, Larson DE, McLellan MD, Mardis ER, et al. VarScan: variant detection in massively parallel sequencing of individual and pooled samples. Bioinformatics (Oxford, England). 2009;25(17):2283-5.
83. Robinson MD, McCarthy DJ, Smyth GK. edgeR: a Bioconductor package for differential expression analysis of digital gene expression data. Bioinformatics (Oxford, England). 2010;26(1):139-40.
84. Li H, Handsaker B, Wysoker A, Fennell T, Ruan J, Homer N, et al. The Sequence Alignment/Map format and SAMtools. Bioinformatics (Oxford, England). 2009;25(16):2078-9.
85. Watanabe K, Taskesen E, van Bochoven A, Posthuma D. Functional mapping and annotation of genetic associations with FUMA. Nature Communications. 2017;8(1):1826.
86. de Leeuw CA, Mooij JM, Heskes T, Posthuma D. MAGMA: Generalized Gene-Set Analysis of GWAS Data. PLOS Computational Biology. 2015;11(4):e1004219.
87. Metsalu T, Vilo J. ClustVis: a web tool for visualizing clustering of multivariate data using Principal Component Analysis and heatmap. Nucleic acids research. 2015;43(W1):W566-W70.
88. Muruganujan A, Ebert D, Mi H, Thomas PD, Huang X. PANTHER version 14: more genomes, a new PANTHER GO-slim and improvements in enrichment analysis tools. Nucleic Acids Research. 2018;47(D1):D419-D26.
89. Swerdlow RH. Mitochondria and Mitochondrial Cascades in Alzheimer's Disease. Journal of Alzheimer's disease : JAD. 2018;62(3):1403-16.

90. Albers DS, Swerdlow RH, Manfredi G, Gajewski C, Yang L, Parker WD, et al. Further Evidence for Mitochondrial Dysfunction in Progressive Supranuclear Palsy. Experimental Neurology. 2001;168(1):196-8.
91. Reas ET. Amyloid and Tau Pathology in Normal Cognitive Aging. The Journal of Neuroscience. 2017;37(32):7561.
92. Tufi R, Gandhi S, de Castro IP, Lehmann S, Angelova PR, Dinsdale D, et al. Enhancing nucleotide metabolism protects against mitochondrial dysfunction and neurodegeneration in a PINK1 model of Parkinson's disease. Nat Cell Biol. 2014;16(2):157-66.
93. Chen Y, Neve RL, Liu H. Neddylation dysfunction in Alzheimer's disease. J Cell Mol Med. 2012;16(11):2583-91.
94. Aguilar BJ, Zhu Y, Lu Q. Rho GTPases as therapeutic targets in Alzheimer's disease. Alzheimer's research & therapy. 2017;9(1):97-.
95. Fransson A, Ruusala, A, Aspenström, P. Atypical Rho GTPases have roles in mitochondrial homeostasis and apoptosis. J Biol Chem. 2003;278(8).
96. Traaseth N, Elfering S, Solien J, Haynes V, Giulivi C. Role of calcium signaling in the activation of mitochondrial nitric oxide synthase and citric acid cycle. Biochimica et Biophysica Acta (BBA) - Bioenergetics. 2004;1658(1):64-71.
97. Burgoyne T, Patel S, Eden ER. Calcium signaling at ER membrane contact sites. Biochimica et Biophysica Acta (BBA) - Molecular Cell Research. 2015;1853(9):2012-7.
98. Chapard C, Meraldi P, Gleich T, Bachmann D, Hohl D, Huber M. TRAIP is a regulator of the spindle assembly checkpoint. Journal of Cell Science. 2014;127(24):5149.
99. Khurana V, Merlo P, DuBoff B, Fulga TA, Sharp KA, Campbell SD, et al. A neuroprotective role for the DNA damage checkpoint in tauopathy. Aging Cell. 2012;11(2):360-2.
100. Ghoshal S, Tyagi R, Zhu Q, Chakraborty A. Inositol hexakisphosphate kinase-1 interacts with perilipin1 to modulate lipolysis. Int J Biochem Cell Biol. 2016;78:149-55.
101. Szijgyarto Z, Garedew A, Azevedo C, Saiardi A. Influence of Inositol Pyrophosphates on Cellular Energy Dynamics. Science. 2011;334(6057):802.
102. Zhu Q, Ghoshal S, Rodrigues A, Gao S, Asterian A, Kamenecka TM, et al. Adipocyte-specific deletion of Ip6k1 reduces diet-induced obesity by enhancing AMPK-mediated thermogenesis. The Journal of clinical investigation. 2016;126(11):4273-88.
103. Crocco P, Saiardi A, Wilson MS, Maletta R, Bruni AC, Passarino G, et al. Contribution of polymorphic variation of inositol hexakisphosphate kinase 3 (IP6K3) gene promoter to the susceptibility to late onset Alzheimer's disease. Biochimica et Biophysica Acta (BBA) - Molecular Basis of Disease. 2016;1862(9):1766-73.
104. Schrauwen P, Schrauwen-Hinderling V, Hoeks J, Hesselink MKC. Mitochondrial dysfunction and lipotoxicity. Biochimica et Biophysica Acta (BBA) - Molecular and Cell Biology of Lipids. 2010;1801(3):266-71.
105. Rentzsch P, Witten D, Cooper GM, Shendure J, Kircher M. CADD: predicting the deleteriousness of variants throughout the human genome. Nucleic Acids Research. 2018;47(D1):D886-D94.
106. Ali AT, Idaghdour Y, Hodgkinson A. Nuclear genetic regulation of human mitochondrial RNA modification. bioRxiv. 2019:666339.
107. Berson A, Nativio R, Berger SL, Bonini NM. Epigenetic Regulation in Neurodegenerative Diseases. Trends in neurosciences. 2018;41(9):587-98.

108. Lin X, Kapoor A, Gu Y, Chow MJ, Peng J, Zhao K, et al. Contributions of DNA Damage to Alzheimer's Disease. Int J Mol Sci. 2020;21(5):1666.
109. Cao J, Zhong MB, Toro CA, Zhang L, Cai D. Endo-lysosomal pathway and ubiquitin-proteasome system dysfunction in Alzheimer's disease pathogenesis. Neurosci Lett. 2019;703:68-78.

APPENDIX

APPENDIX A. IPA ENRICHMENT RESULTS FOR THE DIFFERENTIALLY EXPRESSED GENE-SET.

Ingenuity Canonical Pathways	-log(p-value)	Ratio	Molecules
Reelin Signaling in Neurons	1.84	1.56E-02	HCK,ITGB2
CDP-diacylglycerol Biosynthesis I	1.55	5.00E-02	MBOAT7
Phosphatidylglycerol Biosynthesis II (Non-plastidic)	1.51	4.55E-02	MBOAT7
Tumoricidal Function of Hepatic Natural Killer Cells	1.47	4.17E-02	M6PR
Complement System	1.30	2.78E-02	ITGB2
Triacylglycerol Biosynthesis	1.27	2.56E-02	MBOAT7
Stearate Biosynthesis I (Animals)	1.20	2.17E-02	MBOAT7
Transcriptional Regulatory Network in Embryonic Stem Cells	1.13	1.85E-02	RIF1
Cell Cycle Control of Chromosomal Replication	1.11	1.79E-02	ORC4
MSP-RON Signaling Pathway	1.10	1.72E-02	ITGB2
Regulation of Cellular Mechanics by Calpain Protease	1.06	1.56E-02	CAST
GM-CSF Signaling	1.02	1.43E-02	HCK
Caveolar-mediated Endocytosis Signaling	1.00	1.37E-02	ITGB2
Agrin Interactions at Neuromuscular Junction	0.99	1.32E-02	ITGB2
Macropinocytosis Signaling	0.99	1.32E-02	ITGB2
NF-κB Activation by Viruses	0.96	1.22E-02	ITGB2
HER-2 Signaling in Breast Cancer	0.95	1.19E-02	ITGB2
Fcγ Receptor-mediated Phagocytosis in Macrophages and Monocytes	0.90	1.08E-02	HCK
PPAR Signaling	0.87	9.90E-03	SNW1
Paxillin Signaling	0.85	9.43E-03	ITGB2
Gαs Signaling	0.85	9.43E-03	HCK
Virus Entry via Endocytic Pathways	0.85	9.35E-03	ITGB2
Phagosome Formation	0.82	8.77E-03	ITGB2
Role of Tissue Factor in Cancer	0.82	8.62E-03	HCK
Role of NANOG in Mammalian Embryonic Stem Cell Pluripotency	0.81	8.55E-03	RIF1
Th1 Pathway	0.81	8.55E-03	ITGB2
IL-15 Production	0.81	8.47E-03	HCK
Atherosclerosis Signaling	0.79	8.13E-03	ITGB2
Iron homeostasis signaling pathway	0.77	7.63E-03	HBA1/HBA2
Th2 Pathway	0.76	7.52E-03	ITGB2
PI3K Signaling in B Lymphocytes	0.76	7.46E-03	ATF6B
Phagosome Maturation	0.74	7.09E-03	M6PR
Tec Kinase Signaling	0.69	6.25E-03	HCK
Granulocyte Adhesion and Diapedesis	0.68	6.06E-03	ITGB2
Th1 and Th2 Activation Pathway	0.67	5.99E-03	ITGB2
Xenobiotic Metabolism CAR Signaling Pathway	0.66	5.85E-03	SNW1
Agranulocyte Adhesion and Diapedesis	0.65	5.68E-03	ITGB2
Xenobiotic Metabolism PXR Signaling Pathway	0.65	5.68E-03	SNW1
ILK Signaling	0.63	5.41E-03	ITGB2
RAR Activation	0.62	5.21E-03	SNW1
Clathrin-mediated Endocytosis Signaling	0.62	5.21E-03	ITGB2
Leukocyte Extravasation Signaling	0.62	5.18E-03	ITGB2
IL-8 Signaling	0.61	5.10E-03	ITGB2
Calcium Signaling	0.61	5.05E-03	TPM4
Integrin Signaling	0.59	4.88E-03	ITGB2
EIF2 Signaling	0.58	4.72E-03	RPL18
Sperm Motility	0.58	4.69E-03	HCK
Opioid Signaling Pathway	0.53	4.10E-03	HCK
Systemic Lupus Erythematosus In B Cell Signaling Pathway	0.50	3.77E-03	HCK
Xenobiotic Metabolism Signaling	0.49	3.72E-03	SNW1
Synaptogenesis Signaling Pathway	0.45	3.26E-03	HCK
Breast Cancer Regulation by Stathmin1	0.25	1.72E-03	ANKHD1/ANKHD1-EIF4EBP3

APPENDIX B. SHINYGO ENRICHMENT RESULTS FOR THE UP-REGULATED GENE-SET.

Functional Category	Enrichment FDR	Genes in list	Total genes
Endosome to lysosome transport	0.036911197	2	59
Positive regulation of histone methylation	0.036911197	2	41
Cellular response to extracellular stimulus	0.036911197	3	272
Intrinsic apoptotic signaling pathway in response to DNA damage by p53 class mediator	0.036911197	2	55
Regulation of histone methylation	0.040345816	2	69
Positive regulation of chromatin organization	0.042011958	2	105
Vacuolar transport	0.042011958	2	156
Lysosomal transport	0.042011958	2	115
Intrinsic apoptotic signaling pathway in response to DNA damage	0.042011958	2	117
Response to extracellular stimulus	0.042011958	3	539
Histone methylation	0.042011958	2	151
Peptidyl-lysine methylation	0.042011958	2	139
Cell differentiation	0.042011958	8	4459
Regulation of histone modification	0.042011958	2	146
Positive regulation of histone modification	0.042011958	2	92
Positive regulation of cellular protein metabolic process	0.042011958	5	1680
Histone lysine methylation	0.042011958	2	125
Regulation of RNA splicing	0.042011958	2	145
Regulation of mRNA splicing, via spliceosome	0.042011958	2	103
Cellular developmental process	0.042011958	8	4671
Regulation of mRNA processing	0.042011958	2	148
Positive regulation of protein metabolic process	0.042011958	5	1796
Cellular response to external stimulus	0.042011958	3	343
Intrinsic apoptotic signaling pathway by p53 class mediator	0.042011958	2	87
Negative regulation of binding	0.046599646	2	168

APPENDIX C. GENE-BASED GWAS RESULTS.

ensg	symbol	chr	start	end	strand	posMapSNPs	posMapMaxCADD	minGwasP	IndSigSNPs
Site 585									
ENSG00000164418	GRIK2	6	101846664	102517958	1	1	1.981	NA	rs7754461
ENSG00000047249	ATP6V1H	8	54628117	54756118	-1	4	4.135	NA	rs74399815
ENSG00000067167	TRAM1	8	71485677	71520622	-1	21	12.62	0.0001592	rs16937364
ENSG00000213002	AC120194.1	8	71485681	71486671	1	7	12.04	NA	rs16937364
ENSG00000246366	RP11-382J12.1	8	71520812	71575514	1	42	16.41	8.00E-05	rs16937364
ENSG00000147592	LACTB2	8	71547553	71581409	-1	32	16.41	8.00E-05	rs16937364
ENSG00000221947	XKR9	8	71581600	71702606	1	34	12.17	8.00E-05	rs16937364
ENSG00000197506	**SLC28A3**	**9**	**86890372**	**86955672**	**-1**	**60**	**24.7**	**1.94E-06**	**rs12343928;rs4877837**
ENSG00000110723	EXPH5	11	108376158	108464465	-1	36	8.584	4.54E-06	rs2640758
ENSG00000066933	**MYO9A**	**15**	**72114632**	**72410918**	**-1**	**227**	**18.35**	**4.84E-06**	**rs2034879**
ENSG00000166192	**SENP8**	**15**	**72406599**	**72433311**	**1**	**37**	**13.22**	**4.08E-06**	**rs2034879**
ENSG00000175318	**GRAMD2**	**15**	**72452148**	**72490126**	**-1**	**33**	**16.49**	**9.49E-06**	**rs2034879**
ENSG00000067225	PKM	15	72491370	72524164	-1	26	14.65	3.55E-05	rs2034879
ENSG00000137817	PARP6	15	72533522	72565340	-1	34	12.62	0.0002077	rs2034879
ENSG00000273025	CELF6	15	72559087	72612287	-1	26	15.04	NA	rs2034879
ENSG00000140488	CELF6	15	72577068	72612470	-1	8	15.04	NA	rs2034879
ENSG00000213614	HEXA	15	72635775	72668817	-1	2	5.656	0.0003787	rs2034879
ENSG00000140718	FTO	16	53737875	54155853	1	4	8.108	8.63E-07	rs79977114
ENSG00000132671	SSTR4	20	23016057	23017314	1	2	4.351	NA	rs11696756
ENSG00000178726	THBD	20	23026270	23030378	-1	1	1.48	NA	rs11696756
Site 5520									
ENSG00000176095	**IP6K1**	**3**	**49761727**	**49823975**	**-1**	**58**	**20.7**	**4.67E-07**	**rs9872864**
ENSG00000171865	RNASEH1	2	3592383	3606206	-1	43	6	5.67E-07	rs74621596
ENSG00000185614	FAM212A	3	49840687	49842463	1	5	9.35	5.72E-07	rs9872864
ENSG00000182179	UBA7	3	49842640	49851379	-1	7	9.35	5.72E-07	rs9872864
ENSG00000187492	CDHR4	3	49828165	49837268	-1	10	7.734	5.72E-07	rs9872864
ENSG00000183763	**TRAIP**	**3**	**49866034**	**49894007**	**-1**	**21**	**7.558**	**5.72E-07**	**rs9872864**
ENSG00000161267	BDH1	3	197236654	197300194	-1	7	5.605	3.35E-06	rs2885274
ENSG00000196431	CRYBA4	22	27017928	27026636	1	3	3.193	4.96E-06	rs4822753
ENSG00000100122	CRYBB1	22	26995242	27014052	-1	7	5.467	4.96E-06	rs4822753
ENSG00000226650	KIF4B	5	154393260	154397685	1	15	10.41	1.28E-05	rs6862664
ENSG00000171863	RPS7	2	3622795	3628509	1	21	11.64	1.29E-05	rs74621596
ENSG00000128294	TPST2	22	26921458	26992681	-1	7	5.919	9.46E-05	rs4822753
ENSG00000164076	CAMKV	3	49895421	49907655	-1	11	21.2	0.0004468	rs9872864
ENSG00000164078	MST1R	3	49924435	49941299	-1	14	21.2	0.0005944	rs9872864
ENSG00000164077	MON1A	3	49946302	49967606	-1	9	10.72	0.0013	rs9872864
ENSG00000228008	CTD-2330K9.3	3	49941278	49954370	1	11	10.72	0.0013	rs9872864
ENSG00000173531	MST1	3	49721380	49726934	-1	2	19.37	NA	rs9872864
ENSG00000255767	RP13-512J5.1	2	3579574	3595547	-1	7	3.523	NA	rs74621596
ENSG00000176020	AMIGO3	3	49754267	49761349	-1	19	18.43	NA	rs9872864
ENSG00000173540	GMPPB	3	49754277	49761384	-1	19	18.43	NA	rs9872864
ENSG00000164068	RNF123	3	49726932	49758962	1	21	19.37	NA	rs9872864
Site 7526									
ENSG00000161267	BDH1	3	197236654	197300194	-1	7	5.605	1.88E-07	rs2885274
ENSG00000147459	DOCK5	8	25042238	25275598	1	56	15.73	6.91E-07	rs11779690
ENSG00000176095	**IP6K1**	**3**	**49761727**	**49823975**	**-1**	**58**	**20.7**	**1.03E-06**	**rs9872864**
ENSG00000185614	FAM212A	3	49840687	49842463	1	5	9.35	1.24E-06	rs9872864
ENSG00000182179	UBA7	3	49842640	49851379	-1	7	9.35	1.24E-06	rs9872864
ENSG00000187492	CDHR4	3	49828165	49837268	-1	10	7.734	1.24E-06	rs9872864
ENSG00000183763	**TRAIP**	**3**	**49866034**	**49894007**	**-1**	**21**	**7.558**	**1.24E-06**	**rs9872864**
ENSG00000171587	DSCAM	21	41382926	42219065	-1	34	17.82	4.97E-06	rs2860103
ENSG00000164078	MST1R	3	49924435	49941299	-1	14	21.2	0.002052	rs9872864
ENSG00000164076	CAMKV	3	49895421	49907655	-1	11	21.2	0.002448	rs9872864
ENSG00000164077	MON1A	3	49946302	49967606	-1	9	10.72	0.003515	rs9872864
ENSG00000228008	CTD-2330K9.3	3	49941278	49954370	1	11	10.72	0.003515	rs9872864
ENSG00000173531	MST1	3	49721380	49726934	-1	2	19.37	NA	rs9872864
ENSG00000176020	AMIGO3	3	49754267	49761349	-1	19	18.43	NA	rs9872864
ENSG00000173540	GMPPB	3	49754277	49761384	-1	19	18.43	NA	rs9872864
ENSG00000164068	RNF123	3	49726932	49758962	1	21	19.37	NA	rs9872864

Site 8303									
ENSG00000161267	BDH1	3	197236654	197300194	-1	7	5.605	2.25E-07	rs2885274
ENSG00000176095	**IP6K1**	**3**	**49761727**	**49823975**	**-1**	**58**	**20.7**	**2.56E-07**	**rs9872864**
ENSG00000185614	FAM212A	3	49840687	49842463	1	5	9.35	3.04E-07	rs9872864
ENSG00000182179	UBA7	3	49842640	49851379	-1	7	9.35	3.04E-07	rs9872864
ENSG00000187492	CDHR4	3	49828165	49837268	-1	10	7.734	3.04E-07	rs9872864
ENSG00000183763	**TRAIP**	**3**	**49866034**	**49894007**	**-1**	**21**	**7.558**	**3.04E-07**	**rs9872864**
ENSG00000171865	RNASEH1	2	3592383	3606206	-1	43	6	1.89E-06	rs74621596
ENSG00000164078	MST1R	3	49924435	49941299	-1	14	21.2	9.65E-05	rs9872864
ENSG00000164076	CAMKV	3	49895421	49907655	-1	11	21.2	0.0001499	rs9872864
ENSG00000171863	RPS7	2	3622795	3628509	1	21	11.64	0.0001652	rs74621596
ENSG00000164077	MON1A	3	49946302	49967606	-1	9	10.72	0.0002116	rs9872864
ENSG00000228008	CTD-2330K9.3	3	49941278	49954370	1	11	10.72	0.0002116	rs9872864
ENSG00000173531	MST1	3	49721380	49726934	-1	2	19.37	NA	rs9872864
ENSG00000123066	MED13L	12	116395711	116715143	-1	3	10.31	NA	rs17580851
ENSG00000255767	RP13-512J5.1	2	3579574	3595547	-1	7	3.523	NA	rs74621596
ENSG00000176020	AMIGO3	3	49754267	49761349	-1	19	18.43	NA	rs9872864
ENSG00000173540	GMPPB	3	49754277	49761384	-1	19	18.43	NA	rs9872864
ENSG00000164068	RNF123	3	49726932	49758962	1	21	19.37	NA	rs9872864
Site 9999									
ENSG00000177483	RBM44	2	238707032	238751451	1	22	13.01	3.90E-07	rs76238608
ENSG00000124831	LRRFIP1	2	238536219	238722325	1	25	13.01	3.90E-07	rs76238608
ENSG00000161267	BDH1	3	197236654	197300194	-1	7	5.605	4.47E-07	rs2885274
ENSG00000176095	**IP6K1**	**3**	**49761727**	**49823975**	**-1**	**58**	**20.7**	**1.18E-06**	**rs9872864**
ENSG00000185614	FAM212A	3	49840687	49842463	1	5	9.35	1.27E-06	rs9872864
ENSG00000182179	UBA7	3	49842640	49851379	-1	7	9.35	1.27E-06	rs9872864
ENSG00000187492	CDHR4	3	49828165	49837268	-1	10	7.734	1.27E-06	rs9872864
ENSG00000183763	**TRAIP**	**3**	**49866034**	**49894007**	**-1**	**21**	**7.558**	**1.27E-06**	**rs9872864**
ENSG00000164076	CAMKV	3	49895421	49907655	-1	11	21.2	0.0002059	rs9872864
ENSG00000164078	MST1R	3	49924435	49941299	-1	14	21.2	0.0003178	rs9872864
ENSG00000164077	MON1A	3	49946302	49967606	-1	9	10.72	0.0004537	rs9872864
ENSG00000228008	CTD-2330K9.3	3	49941278	49954370	1	11	10.72	0.0004537	rs9872864
ENSG00000132329	RAMP1	2	238767536	238820756	1	1	0.79	NA	rs76238608
ENSG00000173531	MST1	3	49721380	49726934	-1	2	19.37	NA	rs9872864
ENSG00000176020	AMIGO3	3	49754267	49761349	-1	19	18.43	NA	rs9872864
ENSG00000173540	GMPPB	3	49754277	49761384	-1	19	18.43	NA	rs9872864
ENSG00000164068	RNF123	3	49726932	49758962	1	21	19.37	NA	rs9872864
Site 10413									
ENSG00000176095	**IP6K1**	**3**	**49761727**	**49823975**	**-1**	**58**	**20.7**	**1.88E-07**	**rs9872864**
ENSG00000185614	FAM212A	3	49840687	49842463	1	5	9.35	2.70E-07	rs9872864
ENSG00000182179	UBA7	3	49842640	49851379	-1	7	9.35	2.70E-07	rs9872864
ENSG00000187492	CDHR4	3	49828165	49837268	-1	10	7.734	2.70E-07	rs9872864
ENSG00000183763	**TRAIP**	**3**	**49866034**	**49894007**	**-1**	**21**	**7.558**	**2.70E-07**	**rs9872864**
ENSG00000161267	BDH1	3	197236654	197300194	-1	7	5.605	2.23E-06	rs2885274
ENSG00000147592	LACTB2	8	71547553	71581409	-1	32	16.41	1.35E-05	rs11995646
ENSG00000221947	XKR9	8	71581600	71702606	1	34	12.17	1.35E-05	rs11995646
ENSG00000246366	RP11-382J12.1	8	71520812	71575514	1	42	16.41	1.35E-05	rs11995646
ENSG00000067167	TRAM1	8	71485677	71520622	-1	21	12.62	2.18E-05	rs11995646
ENSG00000164076	CAMKV	3	49895421	49907655	-1	11	21.2	0.0002988	rs9872864
ENSG00000164078	MST1R	3	49924435	49941299	-1	14	21.2	0.0004533	rs9872864
ENSG00000164077	MON1A	3	49946302	49967606	-1	9	10.72	0.0006349	rs9872864
ENSG00000228008	CTD-2330K9.3	3	49941278	49954370	1	11	10.72	0.0006349	rs9872864
ENSG00000173531	MST1	3	49721380	49726934	-1	2	19.37	NA	rs9872864
ENSG00000213002	AC120194.1	8	71485681	71486671	1	7	12.04	NA	rs11995646
ENSG00000176020	AMIGO3	3	49754267	49761349	-1	19	18.43	NA	rs9872864
ENSG00000173540	GMPPB	3	49754277	49761384	-1	19	18.43	NA	rs9872864
ENSG00000164068	RNF123	3	49726932	49758962	1	21	19.37	NA	rs9872864
Site 12146									
ENSG00000161267	BDH1	3	197236654	197300194	-1	7	5.605	5.42E-07	rs2885274
ENSG00000176095	**IP6K1**	**3**	**49761727**	**49823975**	**-1**	**58**	**20.7**	**6.67E-07**	**rs9872864**
ENSG00000185614	FAM212A	3	49840687	49842463	1	5	9.35	8.32E-07	rs9872864
ENSG00000182179	UBA7	3	49842640	49851379	-1	7	9.35	8.32E-07	rs9872864
ENSG00000187492	CDHR4	3	49828165	49837268	-1	10	7.734	8.32E-07	rs9872864
ENSG00000183763	**TRAIP**	**3**	**49866034**	**49894007**	**-1**	**21**	**7.558**	**8.32E-07**	**rs9872864**
ENSG00000147459	DOCK5	8	25042238	25275598	1	56	15.73	3.58E-06	rs11779690
ENSG00000164076	CAMKV	3	49895421	49907655	-1	11	21.2	0.0003932	rs9872864
ENSG00000164078	MST1R	3	49924435	49941299	-1	14	21.2	0.0004168	rs9872864
ENSG00000164077	MON1A	3	49946302	49967606	-1	9	10.72	0.0007223	rs9872864
ENSG00000228008	CTD-2330K9.3	3	49941278	49954370	1	11	10.72	0.0007223	rs9872864
ENSG00000173531	MST1	3	49721380	49726934	-1	2	19.37	NA	rs9872864
ENSG00000176020	AMIGO3	3	49754267	49761349	-1	19	18.43	NA	rs9872864
ENSG00000173540	GMPPB	3	49754277	49761384	-1	19	18.43	NA	rs9872864
ENSG00000164068	RNF123	3	49726932	49758962	1	21	19.37	NA	rs9872864

APPENDIX D. PANTHER ENRICHMENT RESULTS FOR NUCLEAR-ENCODED GENES CORRELATED WITH P9 METHYLATION.

GO biological process complete	Over/Under	Fold Enrichment	p-value	FDR p-value
DNA repair (GO:0006281)	+	2.27	8.71E-05	3.55E-02
cellular response to DNA damage stimulus (GO:0006974)	+	2.22	2.35E-06	1.87E-03
DNA metabolic process (GO:0006259)	+	2.04	7.14E-05	3.15E-02
oxidation-reduction process (GO:0055114)	+	2.01	7.95E-06	5.50E-03
chromosome organization (GO:0051276)	+	1.84	7.43E-05	3.19E-02
organonitrogen compound biosynthetic process (GO:1901566)	+	1.77	2.06E-05	1.09E-02
cellular nitrogen compound biosynthetic process (GO:0044271)	+	1.73	8.83E-06	5.85E-03
nucleobase-containing compound metabolic process (GO:0006139)	+	1.72	5.51E-09	1.10E-05
cellular aromatic compound metabolic process (GO:0006725)	+	1.7	2.50E-09	5.67E-06
cellular nitrogen compound metabolic process (GO:0034641)	+	1.69	1.85E-10	5.90E-07
cellular response to stress (GO:0033554)	+	1.68	1.90E-05	1.08E-02
heterocycle metabolic process (GO:0046483)	+	1.68	6.68E-09	1.18E-05
nucleic acid metabolic process (GO:0090304)	+	1.68	8.35E-07	8.30E-04
small molecule metabolic process (GO:0044281)	+	1.65	5.22E-05	2.44E-02
cellular biosynthetic process (GO:0044249)	+	1.63	2.14E-07	2.83E-04
organic substance biosynthetic process (GO:1901576)	+	1.62	2.35E-07	2.67E-04
biosynthetic process (GO:0009058)	+	1.6	3.08E-07	3.26E-04
organic cyclic compound metabolic process (GO:1901360)	+	1.6	6.35E-08	1.01E-04
gene expression (GO:0010467)	+	1.59	6.40E-05	2.91E-02
organelle organization (GO:0006996)	+	1.46	1.91E-05	1.05E-02
cellular metabolic process (GO:0044237)	+	1.44	1.10E-13	1.75E-09
nitrogen compound metabolic process (GO:0006807)	+	1.44	9.44E-12	5.01E-08
organonitrogen compound metabolic process (GO:1901564)	+	1.41	1.88E-07	2.72E-04
cellular protein metabolic process (GO:0044267)	+	1.39	7.65E-05	3.20E-02
cellular macromolecule metabolic process (GO:0044260)	+	1.39	1.41E-06	1.24E-03
organic substance metabolic process (GO:0071704)	+	1.39	2.24E-11	8.92E-08
metabolic process (GO:0008152)	+	1.39	1.12E-12	8.94E-09
primary metabolic process (GO:0044238)	+	1.39	2.43E-10	6.45E-07
macromolecule metabolic process (GO:0043170)	+	1.37	2.34E-07	2.86E-04
locomotion (GO:0040011)	-	0.34	2.42E-05	1.24E-02
G protein-coupled receptor signaling pathway (GO:0007186)	-	0.28	1.74E-06	1.45E-03
localization of cell (GO:0051674)	-	0.27	1.37E-05	8.40E-03
cell motility (GO:0048870)	-	0.27	1.37E-05	8.09E-03
cell migration (GO:0016477)	-	0.26	3.27E-05	1.63E-02
detection of stimulus (GO:0051606)	-	0.06	9.98E-07	9.34E-04
detection of chemical stimulus involved in sensory perception of smel	-	< 0.01	4.44E-05	2.14E-02
detection of chemical stimulus involved in sensory perception (GO:00	-	< 0.01	1.37E-05	8.73E-03
detection of stimulus involved in sensory perception (GO:0050906)	-	< 0.01	2.77E-06	2.10E-03
detection of chemical stimulus (GO:0009593)	-	< 0.01	6.58E-06	4.75E-03

APPENDIX E. IPA ENRICHMENT RESULTS FOR NUCLEAR-ENCODED GENES CORRELATED WITH P9 METHYLATION.

Ingenuity Canonical Pathways	-log(p-value)	Ratio	z-score
NADH Repair	0.18	3.33E-01	NaN
Ceramide Biosynthesis	0.18	3.33E-01	NaN
Heme Biosynthesis from Uroporphyrinogen-III I	0.18	3.33E-01	NaN
Catecholamine Biosynthesis	0.18	3.33E-01	NaN
Eumelanin Biosynthesis	0.18	3.33E-01	NaN
Phosphatidylcholine Biosynthesis I	0.18	3.33E-01	NaN
Methylmalonyl Pathway	0.18	3.33E-01	NaN
Pentose Phosphate Pathway	0.18	3.33E-01	NaN
N-acetylglucosamine Degradation II	0.18	3.33E-01	NaN
N-acetylglucosamine Degradation I	0.18	3.33E-01	NaN
CDP-diacylglycerol Biosynthesis I	0.23	3.08E-01	0
Ketogenesis	0.23	3.33E-01	NaN
Endoplasmic Reticulum Stress Pathway	0.23	3.08E-01	NaN
UVB-Induced MAPK Signaling	0.25	3.03E-01	1.667
OX40 Signaling Pathway	0.26	3.12E-01	1.342
Ephrin A Signaling	0.26	3.08E-01	NaN
Growth Hormone Signaling	0.27	3.06E-01	1.897
Androgen Biosynthesis	0.27	3.33E-01	NaN
Acyl-CoA Hydrolysis	0.27	3.33E-01	NaN
Calcium Transport I	0.27	3.33E-01	NaN
Role of MAPK Signaling in the Pathogenesis of Influenza	0.27	3.04E-01	NaN
Melanocyte Development and Pigmentation Signaling	0.27	3.04E-01	3.153
TR/RXR Activation	0.27	3.04E-01	NaN
TWEAK Signaling	0.27	3.16E-01	0.816
Apelin Pancreas Signaling Pathway	0.28	3.10E-01	-1
ErbB2-ErbB3 Signaling	0.28	3.08E-01	2.309
Signaling by Rho Family GTPases	0.29	3.03E-01	2.667
ILK Signaling	0.29	3.04E-01	2.785
Xenobiotic Metabolism General Signaling Pathway	0.29	3.06E-01	2.4
Glutathione Redox Reactions I	0.29	3.33E-01	-1
TNFR1 Signaling	0.29	3.12E-01	1.897
Glucose and Glucose-1-phosphate Degradation	0.29	5.00E-01	NaN
Epoxysqualene Biosynthesis	0.29	5.00E-01	NaN
Pentose Phosphate Pathway (Oxidative Branch)	0.29	5.00E-01	NaN
Urea Cycle	0.29	5.00E-01	NaN
Branched-chain α-keto acid Dehydrogenase Complex	0.29	5.00E-01	NaN
Histidine Degradation III	0.29	5.00E-01	NaN
Glycine Cleavage Complex	0.29	5.00E-01	NaN
Glutathione Biosynthesis	0.29	5.00E-01	NaN
UDP-N-acetyl-D-glucosamine Biosynthesis II	0.29	5.00E-01	NaN
GDP-L-fucose Biosynthesis II (from L-fucose)	0.29	5.00E-01	NaN
Ceramide Degradation	0.29	5.00E-01	NaN
Cardiolipin Biosynthesis II	0.29	5.00E-01	NaN
Arginine Degradation I (Arginase Pathway)	0.29	5.00E-01	NaN
1D-myo-inositol Hexakisphosphate Biosynthesis V (from Ins(1,3,4)P3)	0.29	5.00E-01	NaN
Putrescine Biosynthesis III	0.29	5.00E-01	NaN
Lactose Degradation III	0.29	5.00E-01	NaN
S-adenosyl-L-methionine Biosynthesis	0.29	5.00E-01	NaN
DNA Methylation and Transcriptional Repression Signaling	0.29	3.33E-01	NaN

Parkinson's Signaling	0.29	3.33E-01	NaN
Phototransduction Pathway	0.29	3.18E-01	NaN
Thyroid Cancer Signaling	0.30	3.09E-01	2.183
Actin Nucleation by ARP-WASP Complex	0.30	3.11E-01	2.138
Melanoma Signaling	0.30	3.14E-01	1.897
Pancreatic Adenocarcinoma Signaling	0.31	3.10E-01	3.357
Phosphatidylglycerol Biosynthesis II (Non-plastidic)	0.31	3.33E-01	-0.447
Tumoricidal Function of Hepatic Natural Killer Cells	0.31	3.33E-01	NaN
Iron homeostasis signaling pathway	0.32	3.10E-01	NaN
Role of Wnt/GSK-3β Signaling in the Pathogenesis of Influenza	0.32	3.21E-01	1
Assembly of RNA Polymerase II Complex	0.32	3.21E-01	NaN
Mismatch Repair in Eukaryotes	0.32	4.00E-01	NaN
Superpathway of Serine and Glycine Biosynthesis I	0.32	4.00E-01	NaN
Serine Biosynthesis	0.32	4.00E-01	NaN
Glycogen Degradation III	0.32	4.00E-01	NaN
Superoxide Radicals Degradation	0.32	4.00E-01	NaN
Myo-inositol Biosynthesis	0.32	4.00E-01	NaN
Sphingomyelin Metabolism	0.32	4.00E-01	NaN
IL-2 Signaling	0.33	3.17E-01	2.887
Cancer Drug Resistance By Drug Efflux	0.33	3.17E-01	NaN
Role of Osteoblasts, Osteoclasts and Chondrocytes in Rheumatoid Arthritis	0.33	3.09E-01	NaN
Natural Killer Cell Signaling	0.33	3.12E-01	2.858
Cell Cycle Regulation by BTG Family Proteins	0.34	3.33E-01	NaN
CNTF Signaling	0.34	3.24E-01	2.111
HGF Signaling	0.35	3.14E-01	3.273
NF-κB Signaling	0.35	3.12E-01	3.402
Factors Promoting Cardiogenesis in Vertebrates	0.35	3.14E-01	3.411
Role of JAK1, JAK2 and TYK2 in Interferon Signaling	0.35	3.75E-01	NaN
Role of NFAT in Regulation of the Immune Response	0.35	3.12E-01	4.2
Role of BRCA1 in DNA Damage Response	0.36	3.24E-01	-0.447
Oncostatin M Signaling	0.36	3.33E-01	2.121
Inhibition of Angiogenesis by TSP1	0.36	3.33E-01	2.646
Type I Diabetes Mellitus Signaling	0.36	3.20E-01	2.309
Erythropoietin Signaling	0.36	3.20E-01	NaN
LPS-stimulated MAPK Signaling	0.37	3.21E-01	2.668
Regulation of IL-2 Expression in Activated and Anergic T Lymphocytes	0.37	3.21E-01	NaN
Gαs Signaling	0.37	3.18E-01	1.147
Role of p14/p19ARF in Tumor Suppression	0.38	3.57E-01	-1.342
Apelin Endothelial Signaling Pathway	0.38	3.17E-01	2.746
Aldosterone Signaling in Epithelial Cells	0.38	3.16E-01	2.333
SPINK1 General Cancer Pathway	0.38	3.33E-01	2.53
IL-10 Signaling	0.39	3.33E-01	NaN
IL-8 Signaling	0.40	3.16E-01	4.352
Chemokine Signaling	0.40	3.27E-01	1.5
Angiopoietin Signaling	0.40	3.27E-01	1.604
iCOS-iCOSL Signaling in T Helper Cells	0.40	3.27E-01	2.496
IL-3 Signaling	0.40	3.27E-01	3
Cell Cycle: G1/S Checkpoint Regulation	0.41	3.33E-01	0
CTLA4 Signaling in Cytotoxic T Lymphocytes	0.41	3.33E-01	NaN
Endometrial Cancer Signaling	0.42	3.33E-01	2.496

SAPK/JNK Signaling	0.42	3.28E-01	3.441
FAK Signaling	0.43	3.28E-01	NaN
White Adipose Tissue Browning Pathway	0.43	3.25E-01	1.4
mTOR Signaling	0.44	3.20E-01	2.043
Hereditary Breast Cancer Signaling	0.44	3.25E-01	NaN
Regulation of the Epithelial-Mesenchymal Transition Pathway	0.45	3.23E-01	NaN
Aryl Hydrocarbon Receptor Signaling	0.45	3.25E-01	0.408
Integrin Signaling	0.45	3.20E-01	3.888
DNA Double-Strand Break Repair by Non-Homologous End Joining	0.45	4.29E-01	NaN
Prostanoid Biosynthesis	0.45	4.29E-01	NaN
Oleate Biosynthesis II (Animals)	0.45	4.29E-01	NaN
Inflammasome pathway	0.45	4.29E-01	NaN
Lipid Antigen Presentation by CD1	0.45	4.00E-01	NaN
Cleavage and Polyadenylation of Pre-mRNA	0.45	4.00E-01	NaN
NF-κB Activation by Viruses	0.45	3.33E-01	3.3
Arginine Biosynthesis IV	0.46	5.00E-01	NaN
Leukotriene Biosynthesis	0.46	5.00E-01	NaN
Selenocysteine Biosynthesis II (Archaea and Eukaryotes)	0.46	5.00E-01	NaN
Purine Nucleotides De Novo Biosynthesis II	0.46	5.00E-01	NaN
2-oxobutanoate Degradation I	0.46	5.00E-01	NaN
Citrulline-Nitric Oxide Cycle	0.46	5.00E-01	NaN
Folate Transformations I	0.46	5.00E-01	NaN
RAR Activation	0.46	3.20E-01	NaN
IL-6 Signaling	0.46	3.29E-01	3.674
Role of JAK family kinases in IL-6-type Cytokine Signaling	0.46	3.75E-01	NaN
PPAR Signaling	0.48	3.33E-01	-2.683
Mechanisms of Viral Exit from Host Cells	0.49	3.57E-01	NaN
PTEN Signaling	0.50	3.30E-01	-3.024
ATM Signaling	0.50	3.40E-01	0.258
Ovarian Cancer Signaling	0.51	3.33E-01	2
Dolichol and Dolichyl Phosphate Biosynthesis	0.52	1.00E+00	NaN
Proline Biosynthesis II (from Arginine)	0.52	1.00E+00	NaN
Guanine and Guanosine Salvage I	0.52	1.00E+00	NaN
Lipoate Biosynthesis and Incorporation II	0.52	1.00E+00	NaN
Arginine Degradation VI (Arginase 2 Pathway)	0.52	1.00E+00	NaN
5-aminoimidazole Ribonucleotide Biosynthesis I	0.52	1.00E+00	NaN
Coenzyme A Biosynthesis	0.52	1.00E+00	NaN
Acetyl-CoA Biosynthesis III (from Citrate)	0.52	1.00E+00	NaN
D-glucuronate Degradation I	0.52	1.00E+00	NaN
Adenine and Adenosine Salvage III	0.52	1.00E+00	NaN
Spermidine Biosynthesis I	0.52	1.00E+00	NaN
Anandamide Degradation	0.52	1.00E+00	NaN
Thyroid Hormone Biosynthesis	0.52	1.00E+00	NaN
Adenine and Adenosine Salvage I	0.52	1.00E+00	NaN
Galactose Degradation I (Leloir Pathway)	0.52	1.00E+00	NaN
Lanosterol Biosynthesis	0.52	1.00E+00	NaN
Sulfite Oxidation IV	0.52	1.00E+00	NaN
Glycine Betaine Degradation	0.52	1.00E+00	NaN
Tyrosine Degradation I	0.52	1.00E+00	NaN
D-mannose Degradation	0.52	1.00E+00	NaN

Alanine Biosynthesis III	0.52	1.00E+00	NaN
L-serine Degradation	0.52	1.00E+00	NaN
IL-4 Signaling	0.53	3.48E-01	NaN
Gluconeogenesis I	0.55	3.89E-01	-1.89
Antiproliferative Role of TOB in T Cell Signaling	0.55	3.89E-01	0.378
Molecular Mechanisms of Cancer	0.55	3.21E-01	NaN
IL-17A Signaling in Gastric Cells	0.55	4.00E-01	1.342
MIF Regulation of Innate Immunity	0.55	3.75E-01	1
FAT10 Signaling Pathway	0.55	4.17E-01	NaN
Osteoarthritis Pathway	0.56	3.33E-01	1.976
Methylglyoxal Degradation III	0.56	4.44E-01	0
Mitotic Roles of Polo-Like Kinase	0.57	3.64E-01	0
PI3K Signaling in B Lymphocytes	0.57	3.37E-01	3.266
Role of JAK1 and JAK3 in γc Cytokine Signaling	0.57	3.64E-01	NaN
PI3K/AKT Signaling	0.57	3.33E-01	2.556
Induction of Apoptosis by HIV1	0.58	3.59E-01	1.604
Neuregulin Signaling	0.58	3.43E-01	2.183
EGF Signaling	0.58	3.59E-01	2.673
Reelin Signaling in Neurons	0.58	3.37E-01	2.785
Cardiomyocyte Differentiation via BMP Receptors	0.59	5.00E-01	NaN
Assembly of RNA Polymerase I Complex	0.59	5.00E-01	NaN
Phosphatidylethanolamine Biosynthesis II	0.59	5.00E-01	NaN
Urate Biosynthesis/Inosine 5'-phosphate Degradation	0.59	5.00E-01	NaN
Purine Nucleotides Degradation II (Aerobic)	0.59	5.00E-01	NaN
Role of Tissue Factor in Cancer	0.59	3.42E-01	NaN
B Cell Receptor Signaling	0.59	3.37E-01	3.536
Adipogenesis pathway	0.59	3.42E-01	NaN
Renal Cell Carcinoma Signaling	0.60	3.53E-01	2.309
TGF-β Signaling	0.60	3.52E-01	2.668
Rac Signaling	0.60	3.42E-01	3.53
Endocannabinoid Developing Neuron Pathway	0.61	3.41E-01	3.138
Estrogen Receptor Signaling	0.61	3.26E-01	3.873
Telomerase Signaling	0.62	3.48E-01	2.668
Role of PI3K/AKT Signaling in the Pathogenesis of Influenza	0.63	3.79E-01	1.897
TREM1 Signaling	0.63	3.91E-01	2.333
April Mediated Signaling	0.63	3.85E-01	2.53
Toll-like Receptor Signaling	0.64	3.71E-01	2.121
Transcriptional Regulatory Network in Embryonic Stem Cells	0.64	4.00E-01	NaN
MIF-mediated Glucocorticoid Regulation	0.64	4.12E-01	1.134
Apelin Adipocyte Signaling Pathway	0.64	3.64E-01	0
FGF Signaling	0.65	3.62E-01	3.153
Estrogen-Dependent Breast Cancer Signaling	0.65	3.62E-01	3.5
RANK Signaling in Osteoclasts	0.65	3.60E-01	3.153
Apelin Cardiac Fibroblast Signaling Pathway	0.65	4.29E-01	0
Cdc42 Signaling	0.66	3.56E-01	1.5
VEGF Signaling	0.66	3.56E-01	3.5
Creatine-phosphate Biosynthesis	0.66	6.67E-01	NaN
2-ketoglutarate Dehydrogenase Complex	0.66	6.67E-01	NaN
Tetrahydrofolate Salvage from 5,10-methenyltetrahydrofolate	0.66	6.67E-01	NaN
Acetyl-CoA Biosynthesis I (Pyruvate Dehydrogenase Complex)	0.66	6.67E-01	NaN

Molybdenum Cofactor Biosynthesis	0.66	6.67E-01	NaN
Systemic Lupus Erythematosus Signaling	0.70	3.50E-01	NaN
iNOS Signaling	0.71	3.93E-01	1.265
Activation of IRF by Cytosolic Pattern Recognition Receptors	0.71	3.93E-01	1.508
GM-CSF Signaling	0.71	3.70E-01	2.84
PEDF Signaling	0.71	3.64E-01	2.524
BMP signaling pathway	0.71	3.64E-01	2.524
Mouse Embryonic Stem Cell Pluripotency	0.71	3.64E-01	2.683
Role of NANOG in Mammalian Embryonic Stem Cell Pluripotency	0.71	3.64E-01	3.051
HIPPO signaling	0.72	3.61E-01	-0.277
Circadian Rhythm Signaling	0.72	4.09E-01	NaN
HOTAIR Regulatory Pathway	0.74	3.56E-01	3
Mitochondrial Dysfunction	0.74	3.46E-01	NaN
TNFR2 Signaling	0.75	4.38E-01	1.89
Ephrin Receptor Signaling	0.75	3.45E-01	4.226
Role of PKR in Interferon Induction and Antiviral Response	0.78	3.67E-01	1.091
Senescence Pathway	0.78	3.40E-01	2.774
Citrulline Biosynthesis	0.78	6.00E-01	NaN
Bile Acid Biosynthesis, Neutral Pathway	0.78	6.00E-01	NaN
Guanosine Nucleotides Degradation III	0.78	6.00E-01	NaN
Adenosine Nucleotides Degradation II	0.78	6.00E-01	NaN
Necroptosis Signaling Pathway	0.79	3.59E-01	0.378
Huntington's Disease Signaling	0.79	3.39E-01	1.091
NAD Salvage Pathway II	0.82	5.00E-01	-1.342
Superpathway of Citrulline Metabolism	0.82	5.00E-01	0.447
Glycolysis I	0.84	4.44E-01	-0.707
Phagosome Maturation	0.85	3.62E-01	NaN
Leucine Degradation I	0.89	5.71E-01	-1
Th17 Activation Pathway	0.89	4.23E-01	0.302
Apoptosis Signaling	0.90	3.73E-01	-0.6
Inhibition of ARE-Mediated mRNA Degradation Pathway	0.90	3.71E-01	0.392
HIF1α Signaling	0.90	3.77E-01	NaN
Relaxin Signaling	0.91	3.63E-01	2.985
Death Receptor Signaling	0.91	3.91E-01	3.3
Amyloid Processing	0.92	4.00E-01	1
IL-17A Signaling in Airway Cells	0.94	4.05E-01	2.324
IL-23 Signaling Pathway	0.94	4.50E-01	2.333
IL-7 Signaling Pathway	0.94	4.05E-01	3.051
IL-17A Signaling in Fibroblasts	0.94	4.50E-01	NaN
Oxidative Phosphorylation	0.96	3.79E-01	-2.2
Superpathway of Methionine Degradation	0.97	4.71E-01	-0.707
Role of IL-17F in Allergic Inflammatory Airway Diseases	0.97	4.71E-01	2.121
IL-9 Signaling	0.97	4.71E-01	2.828
p38 MAPK Signaling	0.98	3.89E-01	1.886
Ephrin B Signaling	0.98	3.92E-01	3.153
NER Pathway	0.98	3.96E-01	0.775
Methionine Degradation I (to Homocysteine)	1.00	5.56E-01	0.447
Cysteine Biosynthesis III (mammalia)	1.00	5.56E-01	0.447
4-1BB Signaling in T Lymphocytes	1.03	4.55E-01	2.333
NGF Signaling	1.03	3.82E-01	3.674

Chronic Myeloid Leukemia Signaling	1.03	3.87E-01	NaN
UDP-D-xylose and UDP-D-glucuronate Biosynthesis	1.04	1.00E+00	NaN
Glycerol Degradation I	1.04	1.00E+00	NaN
1,25-dihydroxyvitamin D3 Biosynthesis	1.04	1.00E+00	NaN
Hypusine Biosynthesis	1.04	1.00E+00	NaN
Glycerol-3-phosphate Shuttle	1.04	1.00E+00	NaN
Dolichyl-diphosphooligosaccharide Biosynthesis	1.04	1.00E+00	NaN
Glutamine Degradation I	1.04	1.00E+00	NaN
JAK/Stat Signaling	1.06	4.00E-01	2.683
Role of IL-17A in Arthritis	1.06	4.33E-01	NaN
Salvage Pathways of Pyrimidine Ribonucleotides	1.07	4.04E-01	0.471
Inositol Pyrophosphates Biosynthesis	1.07	7.50E-01	NaN
GDP-mannose Biosynthesis	1.07	7.50E-01	NaN
Systemic Lupus Erythematosus In T Cell Signaling Pathway	1.08	3.67E-01	0
IL-17 Signaling	1.08	4.09E-01	NaN
BAG2 Signaling Pathway	1.09	4.44E-01	1.155
PFKFB4 Signaling Pathway	1.09	4.44E-01	2.111
B Cell Activating Factor Signaling	1.09	4.44E-01	3.317
Role of Oct4 in Mammalian Embryonic Stem Cell Pluripotency	1.09	4.44E-01	NaN
Apelin Muscle Signaling Pathway	1.12	5.00E-01	0.707
Role of RIG1-like Receptors in Antiviral Innate Immunity	1.12	5.00E-01	2.449
Glucocorticoid Receptor Signaling	1.13	3.54E-01	NaN
Unfolded protein response	1.15	4.38E-01	2.714
Small Cell Lung Cancer Signaling	1.15	4.13E-01	2.887
FAT10 Cancer Signaling Pathway	1.15	4.38E-01	3.742
Granzyme A Signaling	1.15	6.67E-01	NaN
p53 Signaling	1.18	4.00E-01	0.229
NRF2-mediated Oxidative Stress Response	1.19	3.70E-01	3.962
RAN Signaling	1.20	5.38E-01	2.646
CD40 Signaling	1.20	4.32E-01	2.84
Polyamine Regulation in Colon Cancer	1.20	5.38E-01	NaN
Insulin Receptor Signaling	1.21	3.84E-01	2.921
FLT3 Signaling in Hematopoietic Progenitor Cells	1.24	4.22E-01	2.982
PPARα/RXRα Activation	1.25	3.76E-01	-2.466
Sumoylation Pathway	1.25	4.03E-01	0.447
IL-1 Signaling	1.25	4.03E-01	2.357
EIF2 Signaling	1.25	3.74E-01	2.887
BEX2 Signaling Pathway	1.29	4.15E-01	1.528
IL-22 Signaling	1.29	5.33E-01	2.121
Regulation of eIF4 and p70S6K Signaling	1.32	3.85E-01	2.524
DNA damage-induced 14-3-3σ Signaling	1.32	6.00E-01	NaN
Cell Cycle Control of Chromosomal Replication	1.34	4.80E-01	0.577
Prostate Cancer Signaling	1.34	4.10E-01	NaN
Autophagy	1.38	4.67E-01	NaN
Pyridoxal 5'-phosphate Salvage Pathway	1.40	4.47E-01	0.5
Lymphotoxin β Receptor Signaling	1.47	4.69E-01	2.111
Colanic Acid Building Blocks Biosynthesis	1.53	7.14E-01	-1.342
Assembly of RNA Polymerase III Complex	1.53	7.14E-01	NaN
Acute Myeloid Leukemia Signaling	1.54	4.29E-01	2.837
NAD Phosphorylation and Dephosphorylation	1.56	1.00E+00	NaN

AMPK Signaling	1.66	3.88E-01	1.622
Protein Ubiquitination Pathway	1.80	3.81E-01	NaN
TCA Cycle II (Eukaryotic)	1.88	5.88E-01	0
BER pathway	1.95	8.33E-01	NaN
Sirtuin Signaling Pathway	1.99	3.87E-01	1.155
Endocannabinoid Cancer Inhibition Pathway	2.00	4.19E-01	-2.082
IL-15 Signaling	2.21	4.89E-01	2.985
Hypoxia Signaling in the Cardiovascular System	3.35	5.28E-01	1.265